REVIEW *New Phytol.* (2000), **148**, 195–218

Tansley Review No. 119

Theoretical considerations of optimal conduit length for water transport in vascular plants

JONATHAN P. COMSTOCK[1]* AND JOHN S. SPERRY[2]

[1]*Boyce Thompson Institute for Plant Research, Tower Road, Ithaca, NY 14853, USA*
[2]*Department of Biology, University of Utah, Salt Lake City, UT 84112, USA*

Received 18 April 2000; accepted 22 June 2000

CONTENTS

*Author for correspondence (fax +1 607 254 1242; e-mail jpc8@cornell.edu).

SUMMARY

Vascular plants have shown a strong evolutionary trend towards increasing length in xylem conduits. Increasing conduit length affects water transport in two opposing ways, creating a compromise that should ultimately define an optimal conduit length. The most obvious effect of increased length is to decrease the sequential number of separate conduits needed to traverse the entire pathway, and thereby to reduce the number of wall-crossings and the hydraulic resistance to flow within the xylem. This is an essential evolutionary pressure towards the development of the vessel, a conduit of multicellular origin whose length is not restricted by developmental constraints. The vessel has been an essential component in all plant lineages, achieving transport tissues with very high specific conductivity. A countering effect, however, arises from the partitioning of the cavitation response, a process whereby individual xylem conduits drain of water and lose conducting capacity. Flow in the xylem is down a gradient of negative pressure, which is necessarily most negative in the distal regions (i.e. near the foliage). Cavitation can be caused directly by negative pressures, and results in a total loss of the hydraulic conductance of the individual conduits within which it occurs. If cavitation is triggered by low pressure experienced only at the very distal end of a long conduit, the conduit nevertheless loses its conducting capacity along its entire length. Pathways composed of long conduits will therefore suffer greater total conductance loss for equivalent pressure gradients, because the effects of cavitation are not effectively restricted to the tissue regions within which the cavitation events are generated. By contrast, short conduits can restrict cavitation to distal regions, leaving trunk and root tissues less seriously affected. The increased total conductance loss of a system made entirely of very long conduits translates into a lower maximum rate of water transport in the xylem. The loss in hydraulic capacity associated with failure to partition the flow pathway fully, and locally contain the effects of cavitation, theoretically reaches a maximum of 50% for the extreme case in which a single set of conduits traverses the entire pathway. Shorter conduits confine individual cavitation events to smaller regions and permit the pathway as a whole to have a more gradual conductance loss in conjunction with the pressure gradient. A compromise exists between (1) minimizing total conductance loss from cavitation via fine partitioning of the pathway with many tiers of short conduits, and (2) reducing total wall resistance via coarse partitioning with a few tiers of long conduits. An analysis is presented of the optimal number of end walls (i.e. mean conduit length relative to total pathway length) to maximize transport capacity. The principle of optimal containment of cavitation also predicts that conduits should not be of equal length in all portions of the pathway. The frequency of end walls should rather be proportional to the magnitude of the water-potential gradient at each point, and conduits should be longest in the basal portion (roots) and progressively shortened as they move up the stems to the foliage. These concepts have implications for our understanding of the contrasting xylem anatomies of roots and shoots, as well as the limits to evolution for increased hydraulic conductance per xylem cross-sectional area. They also indicate that to model the hydraulic behaviour of plants accurately it is necessary to know the conduit length distribution in the water flux pathway associated with species-specific xylem anatomy.

Key words: vessel length, water transport, cavitation, anatomical optimization, evolution of xylem, xylem anatomy, hydraulic conductance.

I. INTRODUCTION

1. *The neglected dimension*

This review focuses on understanding the role of xylem conduit length in the hydraulic architecture of plants. Other reviews have dealt extensively with the topics of hydraulic segmentation, branching, redundancy, cavitation and the cohesion–tension mechanism of xylem transport. We discuss these related topics only to the extent that is needed for context, or where vessel length has a prominent role. For more comprehensive treatments of these other issues, the reader is referred to previous reviews (Zimmermann & Brown, 1971; Pickard, 1981; Zimmermann, 1982, 1983; Pallardy, 1989; Tyree & Sperry, 1989; Tyree & Ewers, 1991; Sperry, 1995; Sperry *et al.*, 1996; Tyree, 1997).

A direct evaluation of how conduit length affects flow capacity has received scrutiny only for species with tracheids as the sole type of conducting element (Calkin *et al.*, 1986). This has been due to both technical and theoretical barriers. Accurate measurement of the length of vessels is laborious, and the most common methods are imperfect (Ewers & Fisher, 1989a,b; Tyree, 1992). Consequently our basic knowledge of vessel length is less detailed than that of many other components of xylem anatomy

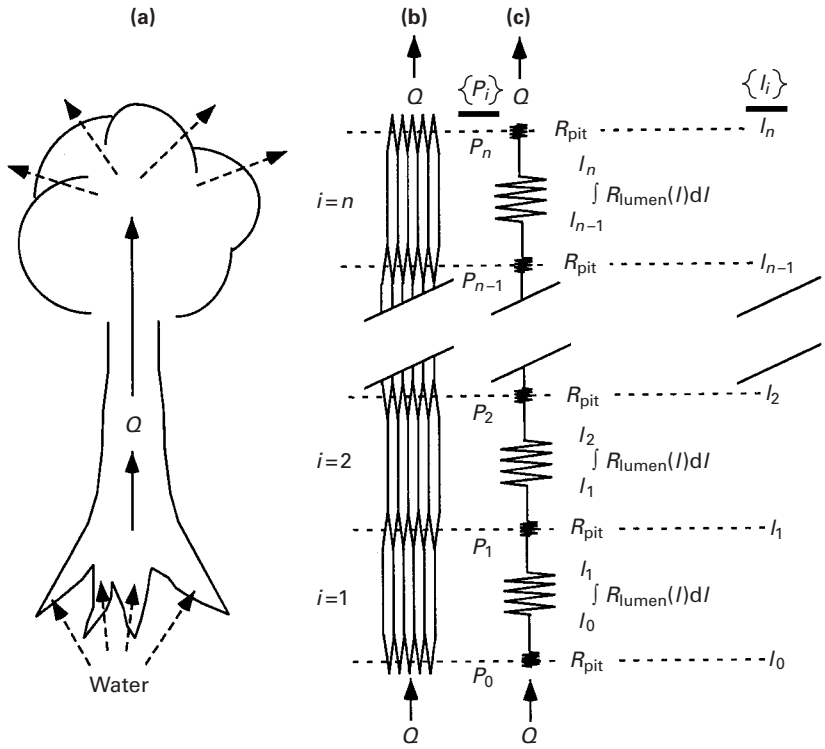

Fig. 1. Idealized flow path divided into n discrete tiers of conduits. (a) The whole plant, engaged in water transport. (b) The flow path described as a set of n conduit tiers. Only five conduits are visible in the drawing for each individual tier, but these represent a full population of perhaps many thousands of conduits at each height. (c) The resistance diagram used to discuss cavitation and flow in a multi-tiered pathway. Shown in the diagram are the alternating pit and lumen resistances of n tiers, which add up to a fixed total resistance of the pathway, R_0, before cavitation. Total lumen resistance can be partitioned unequally among tiers, depending on both individual tier length, as defined by the set of end-wall positions $\{l_i\}$, subdividing total pathway length L, and possible variation in resistivity, $R_{\text{lumen}}(l)$, along the pathway. Branching of the pathway in root and upper canopy are not explicitly recognized in the resistance model, but the relevant effects can be accounted for by variation in $R_{\text{lumen}}(l)$ and relative conduit length, $\{l_i\}$. As used in the text, the labelled resistances define the partitioning of R_0 into a set of resistances, $R_{0,i}$, for each tier. However, the actual resistance under dynamic transport, R_i, will be greater than this because of cavitation, as described by the function $f(P)$. This increase in resistance is calculated separately for each tier as determined by the most negative pressure in each tier, P_i. P_0 allows for variation in soil water potential in different analyses, so that $\{P_i\}$ depends on both soil water status and transport dynamics. During transport, the flux of water through the pathway is Q, and is defined by $Q = \Delta P_i/R_i$. We do not consider issues of capacitance, but instead consider steady-state conditions with Q equal across all tiers. Discussions in the text concern the optimization of n and $\{l_i\}$ with respect to maximizing Q.

and hydraulic architecture (Baas, 1986). Equally important, however, has been incomplete theoretical development quantifying the direct importance of conduit length to transport processes. In this review we outline the broad patterns of conduit length over evolutionary time and across modern ecological groups. We also present a theoretical framework that integrates vessel length into quantitative estimates of hydraulic limitations to plant water-use and growth. The concepts and approaches to estimating maximum transport capacity as limited by xylem sap cavitation are dealt with in a standard fashion (Tyree, 1997; Sperry *et al.*, 1998), but the explicit inclusion of the way in which conduit length modifies the cavitation response leads to new insights. We hope that this discussion will draw the attention of future studies to this often-neglected dimension.

2. *Basic concepts*

(a) *The heuristic notion of vessel-tiers.* The flow path of a plant is typically composed of many thousands of xylem conduits. At any given height there may be thousands of conduits in a single cross section. Conduits within a single section are usually not all the same length but in fact have characteristic length frequency profiles that are almost always skewed towards shorter conduits (Zimmermann & Brown, 1971; Zimmermann & Jeje, 1981; Zimmermann, 1983; Ewers & Fisher, 1989b; Ewers *et al.*, 1990). However, a representative length can be determined from such a frequency histogram and our principal concern here is not with length variation within a single axis segment but rather in the average number of wall-crossings needed to traverse the pathway,

Table 1. *List of symbols and abbreviations used in water-transport studies*

Variable	Units	Description
i	–	Index variable for tier number ranging from 1 to n
K	kg MPa^{-1} s^{-1}	Hydraulic conductance of whole pathway
K_0	kg MPa^{-1} s^{-1}	Hydraulic conductance of whole pathway before cavitation
K_i	kg MPa^{-1} s^{-1}	Hydraulic conductance of the ith tier
$K_{0.i}$	kg MPa^{-1} s^{-1}	Hydraulic conductance of the ith tier before cavitation
$K_{\mathrm{lumen}.i}$	kg MPa^{-1} s^{-1}	Inverse of $\int R_{\mathrm{lumen}}(l)\mathrm{d}l$ for the ith tier after cavitation
$K_{\mathrm{pit}.i}$	kg MPa^{-1} s^{-1}	Inverse of R_{pit} after cavitation
R_{pit}	MPa s kg^{-1}	Pit-membrane resistance of crossing all the end walls of a single tier of conduits
$R_{\mathrm{lumen}}(l)$	MPa s kg^{-1} m^{-1}	Function describing lumen resistivity (i.e. length-specific resistance) at point l along the flow pathway
R	MPa s kg^{-1}	Total resistance after cavitation (ΣR_i), reciprocal of K
R_0	MPa s kg^{-1}	Total resistance before cavitation ($\Sigma R_{0.i}$), reciprocal of K_0
$R_{0.i}$	MPa s kg^{-1}	Resistance of ith tier before cavitation ($R_{\mathrm{pit}}+\int R_{\mathrm{lumen}}(l)\mathrm{d}l$ over pathway segment L_i, reciprocal of $K_{0.i}$
R_i	MPa s kg^{-1}	Resistance of ith tier after cavitation ($R_{0.i}/f(P_i)$), reciprocal of K_i
$\partial R/\partial L_i$	MPa s kg^{-1} m^{-1}	Partial derivative of total pathway resistance after cavitation with respect to an incremental length-change of the ith tier
C	m	Conduit radius
D	m	Diameter of pore in pit-membrane
L	m	Length of total pathway
L_i	m	Length of the ith tier
l	m	Linear position along length L
n	–	Number of conduit tiers in flow pathway
$n_{Q\max}$	–	Optimal n maximizing Q at given $\int R_{\mathrm{lumen}}(l)\mathrm{d}l/R_{\mathrm{pit}}$
OCLD	–	Optimal conduit tier-length distribution
Q	kg s^{-1}	Water flux
Q_{guess}	kg s^{-1}	Value of Q to be tested by iterative routine for a viable water potential gradient and sustainable cavitation while numerically searching for $Q_{\max}$
$Q_{\max}$	kg s^{-1}	Maximal water flux before cavitation collapse for any defined value of n and conduit tier-length distribution $\{l_i\}$
$Q^*_{\max}$	kg s^{-1}	Maximal water flux based on Eqn 8. The cavitation dynamics are infinitely partitioned as though $n = \infty$, but K_0 is defined independently of nR_{pit}
$Q^n_{\max}$	kg s^{-1}	$Q_{\max}$ as a function of n, with $\{l_i\}$ always an OCLD, and n controlling both Θ and nR_{pit}
$Q^{n=\mathrm{opt}}_{\max}$	kg s^{-1}	$Q^n_{\max}$ with n optimal for $\int R_{\mathrm{lumen}}(l)\mathrm{d}l/R_{\mathrm{pit}}$
P	MPa	Water pressure
P_0	MPa	Water pressure of source water entering plant flow pathway
P_i	MPa	Water pressure of distal end of the ith conduit tier
$P_{k=0}$	MPa	Water pressure at which total cavitation is reached
$\mathrm{d}P/\mathrm{d}l$	MPa m^{-1}	Rate of change in P with distance along pathway
ΔP	MPa	Discrete decrease in P over the entire water transport pathway
ΔP_i	MPa	Discrete decrease in P over the ith conduit tier
$f(P)$	–	Fractional conductivity left after cavitation
η	MPa s	Viscosity of water
ρ	kg m^{-3}	Density of water
σ	MPa m	Surface tension of water
Θ	–	Fractional reduction in $Q_{\max}$ due solely to the lack of containment of cavitation at the sites of origin

and how the mean length of all conduits affects the containment of xylem failure via cavitation (Tyree & Sperry, 1989). Water must pass from one set of conduits to the next in longitudinal series to move from the soil to the foliage, and we define the number of tiers of conduits as the total pathway length divided by the mean conduit length. We refer to tiers of conduits as though they were organized discretely with the ends of all conduits in a given tier beginning and ending in the same cross sections (Fig. 1b). This will simplify discussion and numerical evaluation, but the reader should understand that, in most plants, the ends of individual conduits are more often randomly distributed longitudinally than lined up in a transverse plane. In addition, the 'end' of a conduit is really an extended region of overlap with adjacent conduits (Zimmermann & Brown, 1971). The degree to which these simplifications might affect conclusions is discussed. We focus, in our review and analysis, on the influence of conduit tier structure on the conducting capacity of plant xylem. We analyse how conducting capacity can be optimized by varying the number of conduit tiers in a plant pathway, and whether tiers should all have

the same length, or whether individual tier length should vary in a predictable manner along the flow path from roots to leaves.

(b) *Ohm's law*. The Ohm's law analogy is generally used to model the steady-state transport of water in plant xylem (Passioura, 1988; Tyree & Ewers, 1991):

$$Q = K\Delta P, \qquad \text{Eqn 1}$$

(Q, water flow through the xylem; K, is hydraulic conductance; ΔP is total pressure drop across the flow path.) The term K_0 will be used to refer to the saturated K when there is no cavitation and all conduits are functional.

(c) *Conductances, resistances and resistivities*. Resistance and conductance units are simply the reciprocals of each other: $R = 1/K$. Any expression in conductance units can be rewritten in terms of the equivalent resistances, and vice versa. Each unit has its preferential application, however. Flow, as expressed in Eqn 1, is directly proportional to conductance. Transport capacity and loss of capacity due to cavitation are most commonly reported in the literature in conductance units. However, when a complex pathway such as multiple discrete tiers of conduits is being analysed, resistances in series are simply additive, whereas equivalent expressions in conductance units are more complex. The related term, resistivity, is defined as the length-specific resistance of a pathway, and must be integrated over the pathway length to determine total pathway resistance.

(d) *Lumen and pit resistances*. The summation of resistances in series associated with moving water through plant xylem with multiple tiers of conduits includes both the resistances of the conduit lumen and those associated with crossing from one conduit to the next through the interconduit pits. We define a total wall-crossing resistance, R_{pit}, associated with all water in the pathway moving from one conduit tier to the next (i.e. all conduits in a cross section are included, and all water crosses one conduit wall, once). Similarly, we define a resistivity, $R_{\text{lumen}}(l)$, to represent the combined lumen of all conduits in any given cross section. Note that the lumen resistivity is defined as a function of of the linear position, l, along the pathway, and need not be constant. To determine the initial hydraulic conductance of an entire pathway (before any cavitation) we must multiply R_{pit} by the number of conduit tiers (n), and integrate $R_{\text{lumen}}(l)$ over the total pathway length (L) (Fig. 1c):

$$K_0 = \frac{1}{R_0} = \frac{1}{nR_{\text{pit}} + \int_0^L R_{\text{lumen}}(l)\mathrm{d}l} \qquad \text{Eqn 2}$$

(e) *The importance of conduit radius and length in conductance*. One of the most important determinants of variation in hydraulic conductance between different species has been the dependence of the lumen resistivity on the fourth power of conduit radius (C) (Zimmermann, 1983; Vogel, 1988; Tyree & Ewers, 1991). Because the cross-sectional space occupied by a conduit is proportional only to C^2, but resistivity declines as the fourth power, large-diameter conduits are far more efficient in water transport per unit of ΔP. $R_{\text{lumen}}(l)$ is therefore related to both the number of conduits in parallel and the individual lumen radii (as expressed by the Hagen–Poiseuille equation):

$$R_{\text{lumen}}(l) = \frac{8\eta}{\pi\rho\Sigma C^4} \qquad \text{Eqn 3}$$

(η, the dynamic viscosity of water; ρ, the density of water, which is included to convert volume to mass flow, to be consistent with our units for Q.)

II. EVOLUTIONARY TRENDS IN CONDUIT DIMENSIONS

1. *Nature and origin of xylem conduits*

Photosynthesis, like most of the central pathways of metabolism, arose in the seas; the invasion of terrestrial environments was associated with the evolution of new capabilities for water management and the erect habit. Many of the anatomical features needed to sustain complex land plants evolved during the Ordovician and Silurian periods (Edwards, 1993, 1996; Bateman *et al*., 1998), including a water-resistant cuticle, stomatal pores and primitive conducting strands, making it possible for small plants to control their water content in terrestrial environments.

A key to the evolution of larger, erect plant forms was the origin of highly specialized vascular tissues permitting the long-distance transport of water. This was apparently a difficult and revolutionary innovation, and all vascular plants are thought to be monophyletic (Kenrick & Crane, 1997; Doyle, 1998). In the upper Silurian we find the first appearance of xylem conduits in the form of tracheids (Edwards & Davies, 1976): elongated single cells specialized for transporting water under negative pressure. To avoid implosion, the walls of tracheids include secondary layers for thickening and are impregnated with the stiffening agent lignin. Lignified and thickened walls are both characteristic of vascular plants (Gross, 1980; Edwards, 1993; Doyle, 1998); in modern plants they are found in a wide range of tissues, where they aid in protection and support as well as transport. However, thick lignified walls might first have evolved in response to the collapsing forces of water under tension in the early conduits (Raven, 1987; Bateman *et al*., 1998). In the earliest vascular plant fossils, thickened, lignified walls are found exclusively in central conducting strands rather than peripheral locations, where they would have contributed much more

effectively to support (Niklas, 1997). Nevertheless, lignin and secondary wall specializations made possible the development of xylem tissues that are capable of the dual functions still performed by the tissue in extant species: (1) water transport *under negative pressure* in specialized conduits, and (2) withstanding the compressional forces of erect morphologies and increasing size (Barghoon, 1964). These new capacities unleashed the evolution of modern plant habits as different lineages lifted their photosynthetic and reproductive organs higher and higher above ground.

The immature, living stages of xylem conduit ontogeny produce the intricate cell wall structure of contrasting thin porous regions of exposed primary wall surrounded by thickened lignified regions of secondary wall deposition that are essential to function. However, at maturity the conduit cells die, leaving open, unobstructed lumens for water flow under negative pressure. Implosion is prevented by the thick, lignified regions of the wall, whereas flow between adjacent conduits (and other neighbouring cell types) occurs through the thin and porous 'pits' of the common wall. These pits consist of a porous 'pit membrane' derived from the compound middle lamella of the adjacent cells, which divides opposing pit 'chambers' formed by the openings in the secondary walls. The over-arching secondary walls surrounding the chambers of bordered pits allow maximum pit membrane surface area without unduly weakening the strength of the wall against implosion (Mauseth, 1988).

The xylem conduits thus form an extensive system of capillaries, each closed at both ends, that overlap and form a network ramifying throughout the plant body. For long-distance transport, water flows most of the time in the large, unobstructed lumen of the capillaries, but must also cross through interconduit pits at a frequency determined by the length of the individual conduits relative to the overall pathway. Consequently, the hydraulic resistance to flow in the xylem has two distinct components: (1) resistance to flow in the lumen and (2) crossing the thin, but much more restrictive, microporous pit membranes of the interconduit pits (Eqn 2).

2. *Increasing hydraulic conductance with increasing diameter and length*

(a) *Evolutionary trends in tracheid dimensions*. If we look at the early fossil record, there is a trend towards ever more specialized tracheids permitting more efficient conducting tissues (Niklas, 1985). The most easily interpreted feature of this record is the increase in tracheid diameter with time. In the earliest erect plants, mean tracheid diameter increases severalfold from the Upper Silurian to the Upper Devonian (Niklas, 1985). From the Hagen-Poiseuille equation (Eqn 3), a doubling in diameter translates to a decrease in lumen resistivity to 1/16. Associated with the increase in diameter is an implied increase in length (Bailey, 1953), which would decrease the contribution of R_{pit} to total xylem resistance (Eqn 2) by reducing the number of times that water must cross between conduit lumens.

Many extant taxa still rely exclusively on tracheids for water transport, and by the end of the Devonian, tracheid diameter in several lineages had reached a plateau at values comparable to those in modern forms (Niklas, 1985). The limitation to this evolutionary trend is illustrated by recent studies comparing the conducting capacity of the lumen with that of the interconduit pits connecting adjacent lumens through overlapping walls (Gibson *et al.*, 1984; Calkin *et al.*, 1986; Schulte & Gibson, 1987; Veres, 1990). These areas of overlap might actually span up to 50% of the total tracheid length (Schulte *et al.*, 1987), with pit membranes occupying up to 80% of the contact zone. Nevertheless, as conduit radius increases, the capacity of the lumen for water transport increases under a fourth-power law, whereas the contact surface area determining the total interconduit pit transport capacity increases only linearly. Consequently, at large conduit diameters, the pit resistance becomes increasingly limiting, contributing 50% or more of the total hydraulic resistance of the pathway (Calkin *et al.*, 1986). Selective pressure to reduce pit resistance presumably resulted in the evolution of longer xylem conduits, to reduce the number of wall crossings in the flow pathway (Eqns 2 and 3).

However, it seems that developmental constraints put an upper limit of only a few centimetres (and more commonly a few millimetres) on the potential length of individual tracheids, and thereby on the ultimate conducting efficiency that can be attained by xylem tissues composed only of tracheids (Bailey, 1953). Moreover, in wood composed exclusively of tracheids, the same relatively homogeneous tissue is performing both transport and support functions. In the Coniferales, one of the most arborescent groups using only tracheids for water transport, the tracheids are actually rather short and narrow compared with tracheids of many herbaceous taxa, and have relatively thick walls to enhance support (Bailey, 1953).

(b) *Origin of the vessel*. The solution to this limitation on water transport was the evolution of a new type of conduit, the vessel, but this new structure is not clearly present in the fossil record until the sudden proliferation of the gnetophytes and, especially, the angiosperms, in the Jurassic and Cretaceous. Vessels, like tracheids, are dead at maturity and form an extensive, overlapping system of micro-capillaries. Unlike tracheids, vessels are multicellular in origin. They are composed of hundreds or thousands of individual 'vessel

elements' stacked in vertical files. Vessel members evolved from tracheids by the progressive enlargement of interconduit pits and the degradation of pit membranes to form open perforation plates (Bailey & Tupper, 1918). The individual members at the top and bottom of the vessel retain their end walls and define the total length of the vessel. It is important to realize that, although these intermittent end walls define the length of the vessel, water, in moving from one vessel to the next, does not pass primarily through the end walls themselves, but rather through extensive regions of overlap (Zimmermann, 1978). Like tracheids, vessels must overlap for a large fraction of their length to provide surface area for interconduit pits, but, in contrast with tracheids, vessels can produce unobstructed lumen of indefinite length, tremendously reducing the number of pit-membrane crossings in the flow path. This increased conduit length made possible xylem tissues with unprecedented lumen diameter and conducting efficiency (Ewers, 1985), and the development of more complex xylem tissues with vessel elements specialized for water conduction and fibres specialized for support (Bailey & Tupper, 1918; Baas, 1986). Vessels apparently evolved independently in several vascular lineages (Bailey, 1953; Gifford & Foster, 1989). However, they are most abundant and specialized in structure within the angiosperms, in which they have had an important role in the morphological plasticity and adaptive radiation of this group (Cronquist, 1988).

Modern plants show a tremendous range in the dimensions of vessels. Vessel radii can vary by as much as two orders of magnitude, from 2 or 3 μm up to 250 μm in different plant species (Ewers & Cruziat, 1991). Conduits with smaller radii are more resistant to cavitation by freezing stress (Hammel, 1967; Ewers, 1985; Lo Gullo & Salleo, 1993; Davis *et al*., 1999) and there is a strong correlation of decreasing conduit radius with latitude, or increased radius with specialized habits requiring very high conducting efficiency per unit stem cross section, such as lianas (Carlquist, 1975; Baas, 1986; Ewers *et al*., 1990; Ewers & Fisher, 1991; Chiu & Ewers, 1992). Vessels show an even greater range of lengths, spanning four orders of magnitude from 5 mm to 5 m (Zimmermann & Jeje, 1981). It seems likely that the much greater range in length than in radius is due in part to the extreme efficiency of lumen transport in large diameter vessels, and the need to reduce pit resistance in parallel to realize this benefit (Eqns 2 and 3).

3. *Functional limitations to increasing vessel length*

(a) *Safety versus efficiency*. Many modern angiosperms exist in which a few individual vessels can span the entire height of a tall tree or vine (Handley, 1936; Greenidge, 1952; Zimmermann & Jeje, 1981; Ewers *et al*., 1991). However, such vessels are rare, even in the plants in which they occur, and represent an extreme tail on the distribution of vessel lengths in the plant body, most of which are relatively short. Are there liabilities to excessive vessel length that limit the directional evolution for more efficient conduits? Earlier work on this issue emphasized a compromise between safety from damage on the one hand, and hydraulic efficiency on the other (Zimmermann, 1983). The length of the conduits has major implications for methods of control of damage and leakage in the transport system.

It is the nature of transport under negative pressure that air will tend to leak into the conduit network rather than the fluid leaking out. In the thickened wall regions, entry of air into the conduit lumen is unlikely owing to the impregnation of the wall matrix with lignin. Any pores that happened to be continuous through the thick wall are probably less than a few nanometers in diameter and capable of excluding air entry by capillary force (Oertli, 1971; Pickard, 1981). Inevitably, however, the walls of some conduits become damaged during normal plant development. This happens, for example, by the rupture of protoxylem conduits during organ expansion, and by the abscission of leaves and fine roots. In addition, conduits become injured by herbivory, pathogen action and storm damage.

The ruptured conduits allow air to leak in because their lumen diameters are much too large to establish sufficient capillary force to hold water under significant negative pressure. As the water is withdrawn from the damaged conduit, the conduit becomes entirely filled with air or embolized. In this circumstance, the interconduit pits reveal their essential function as check valves, anchoring the air–water meniscus by capillary forces in the relatively small pores of cellulosic mesh of the pit membranes. If the pit membranes have a torus–margo structure (as in many gymnosperms), capillary forces in the porous and peripheral margo aspirate the membrane so that the pit opening becomes blocked by the central thickened torus. By either mechanism, the check-valve function of the interconduit pits allows negative pressures to persist in the undamaged conduit system (Zimmermann, 1983).

Because damage at a point source in the conduit network causes dysfunction in a large fraction, but not all, of the conduits at a single level in the pathway, the full magnitude of lost hydraulic conductance in the pathway as a whole is highly sensitive to conduit length. For example, if a point injury damaged 50% of the conduits, and a single set of conduits traversed the entire flow pathway, then total conducting ability would be reduced by a full 50%. By contrast, if 10 conduit lengths were needed to traverse the entire pathway, and the injury was sufficiently local to affect only one of these 10 tiers of conduits with the same 50% damage, then the loss of

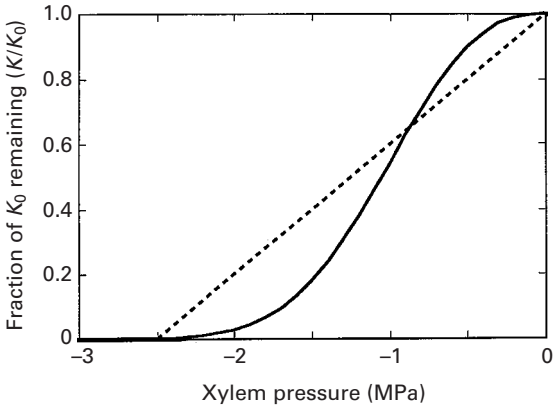

Fig. 2. Cavitation vulnerability functions showing the rate of loss in total conductance with increasingly negative xylem pressure. Dotted line, linear vulnerability function, $K/K_0 = 1 + mP$ with $m = 0.4$; solid line, Weibull function, $K/K_0 = \exp[-(-P/d)^c]$, with $d = 1.2$ and $c = 2.5$.

hydraulic conductance to the entire pathway would be just under 9%. Although the level of physical damage is the same in both cases, the difference in effect is a simple consequence of containment of the damage to a local region by short conduits, and the way in which local resistances are additive in series (Zimmermann, 1983). Thus, conducting systems composed of extremely long conduits are extremely susceptible to failure from mechanical point-injuries and pathogen attack anywhere along the pathway (see also Tyree *et al.*, 1994a). Interestingly, some of the most marked examples of species decline from vascular disease have occurred in ring-porous trees in which the functional xylem is composed of a relatively small number of vessels with large diameters and great length, namely American elm and chestnut (Zimmermann, 1983).

(b) *Containment of cavitation and embolism.* There is, however, a less obvious but more ubiquitous problem with long xylem conduits than sensitivity to injury. This arises because the transport system is subject to intrinsic dysfunction from cavitation. Cavitation is the vapourizing of liquid xylem sap that is under negative pressure; it results in a gas-filled or embolized conduit. As pressures become increasingly negative during water stress, cavitation occurs conduit by conduit and there is a progressive loss of hydraulic conductivity. The rate of conductance loss by whole tissues is usually characterized by a 'vulnerability curve' that describes the cumulative loss of xylem conductance with declining negative pressure (Fig. 2). Cavitation reduces the initial conductance, and the effects are usually described in terms of fractional loss as a function of negative pressure:

$$\frac{K}{K_0} = f(P) \qquad \text{Eqn 4}$$

Both the exact shape of $f(P)$ and the range of P over which loss occurs is highly species-specific. Significant cavitation can occur in plants under natural water stress conditions (Yang & Tyree, 1993; Mencuccini & Comstock, 1997; Kolb & Sperry, 1999a; Hacke *et al.*, 2000).

There is evidence that the cause of cavitation is the failure of the check-valve function of interconduit pits in confining gas to embolized conduits (Crombie *et al.*, 1985; Sperry & Tyree, 1988, 1990; Jarbeau *et al.*, 1995; Sperry *et al.*, 1996). These pits can exclude an air/water interface up to a critical negative xylem pressure (P_{critical}) at which point air leaks through the seal and nucleates cavitation in the adjacent conduit. For those non-gymnosperm pits in which the sealing is apparently by capillary action alone, P_{critical} is given by the capillary equation (Tyree & Sperry, 1989):

$$P_{\text{critical}} = \frac{-\cos(\alpha)4\sigma}{D} \qquad \text{Eqn 5}$$

(D, is the largest pore diameter crossing the pit membrane or conduit wall; σ, the surface tension of water (7.28×10^{-8} MPa m at 20°C); α, the contact angle between water and the pore wall, which is usually assumed to be zero for cellulosic wall material.) Plants from different ecological settings typically have minimum values of xylem pressure reaching perhaps −1.0 MPa in mesophytes, and as low as −6 or −7 MPa in some xerophytes. This would require values of D smaller than 0.3–0.05 μm, respectively ($\alpha = 0$). Even for the mesophyte expecting minimal stress from negative pressures, this corresponds to pore sizes determined for the pit membranes (Sperry & Tyree, 1988; Jarbeau *et al.*, 1995), but is much smaller than the open lumen of the conduit itself, which ranges from 5 to 500 μm in diameter. D is apparently a feature of conduit structure that is highly adaptable in modern plants, because cavitation pressures show strong patterns of variation between species, often correlated with the aridity of different habitats (Tyree *et al.*, 1994b; Jarbeau *et al.*, 1995; Linton *et al.*, 1998; Kolb & Sperry, 1999a). In gymnosperm pits, P_{critical} is probably related to the elasticity of the pit membrane because evidence suggests that slippage of the torus from its blocking position over the pit aperture allows air through to cause cavitation (Sperry & Tyree, 1990).

There is stark conflict between the two functions of interconduit pits. On the one hand they must be as permeable as possible to the passage of water to minimize R_{pit} (Eqn 2) and facilitate the supply of water to foliage. This would be achieved by maximizing D of pit membrane pores (Eqn 5). On the other hand, D cannot be too large or these same pits will be too permeable to an air/water interface. The same conflict presumably occurs for gymnosperm pits, in which a greater permeability of the torus–margo pit membrane to water might be achieved at the expense of a weaker pit membrane that allows

more ready slippage of the torus (Sperry & Tyree, 1990). The end result of this compromise between hydraulic efficiency and safety should be a pit structure that is only as protective of cavitation as it has to be to avoid excessive cavitation by the xylem pressures experienced by the plant in its habitat.

How might dysfunction by cavitation constrain conduit length? Because water transport is driven by a gradient in decreasing pressure, pressures are lowest and cavitation is more likely in the distal regions of the plant (assuming equal resistance to cavitation along the flow path). If conduits are short, high levels of cavitation might be restricted to these distal regions (Salleo & Lo Gullo, 1983; Salleo, 1984). If they are very long, conductance loss might extend back along the pathway for great distances and include regions where the local pressures were not low enough to cause cavitation. Therefore, the cavitation vulnerability curve, the pressure gradient associated with transport, and the length of the xylem conduits interact to determine a degree of conductance loss and the transport capacity of the conduit network.

III. MAXIMUM XYLEM TRANSPORT IN THE PRESENCE OF CAVITATION

1. *Cavitation is linked to the driving force for transport*

The vulnerability of the xylem to cavitation limits the sustainable negative pressures within it, and therefore limits the maximum driving force for transport (ΔP) and the maximum flow rate (Q_{max}) (Tyree & Sperry, 1988; Sperry *et al.*, 1998). The actual flow rates can approach Q_{max} on a daily or seasonal basis, suggesting that this hydraulic limitation is important in limiting gas exchange in many species (Tyree & Sperry, 1988; Sperry *et al.*, 1993; Tyree *et al.*, 1993, 1994b; Cochard *et al.*, 1995; Saliendra *et al.*, 1995; Lu *et al.*, 1996; Meinzer *et al.*, 1997; Kolb & Sperry, 1999b).

All of these analyses, whether evaluating Q_{max} itself, or ΔP required at a defined, submaximal Q, require a simultaneous solution of Eqns 1 and 4. Depending on the complexity of the function $f(P)$, this is sometimes done analytically or else by using numerical approximations. Many studies have divided the overall pathway into two or more sequential regions on the basis of concepts of hydraulic segmentation in either $R_{lumen}(l)$ (Zimmermann & Brown, 1971; Zimmermann, 1983; Ewers & Zimmerman, 1984; Salleo, 1984; Sperry, 1986; Sellin, 1988; Lo Gullo, 1989; Cochard *et al.*, 1992; Meinzer *et al.*, 1992; Yang & Tyree, 1994; Joyce & Steiner, 1995; Aloni *et al.*, 1997) or $f(P)$ (Tyree *et al.*, 1993; Mencuccini & Comstock, 1997; Sperry & Ikeda, 1997; Tsuda & Tyree, 1997; Linton *et al.*, 1998; Linton & Nobel, 1999) in different parts of the pathway. This usually amounts to dividing the pathway into units defined by organs (i.e. root, trunk, branch, twig and petiole).

However, most of these analyses have not directly addressed the importance of conduit length. Consider a plant in which all conduits are as long as the flow path from roots to leaves. As the flow rate through the xylem is increased and distal pressures become more negative, air-seeding events precipitating cavitation will occur first in the leaves and distal twigs, yet the consequent reduction in hydraulic conductivity will extend all the way to the roots. In consequence, the reduction in total conductance and Q_{max} will be substantially greater than in a plant with shorter xylem conduits that confine the loss of conductivity to the distal portion of the pathway. Conduit length might, in many instances, correlate with other aspects of hydraulic segmentation, but cannot be assumed to do so a priori (Aloni & Griffith, 1991).

2. *Transport models and extreme assumptions about conduit length*

Although previous analyses of Q_{max} have not directly addressed the importance of conduit length, the partitioning of the flow pathway into separate conduit populations is the universal condition of all vascular plants. Depending on species' anatomy, the number of conduit lengths (n) needed to traverse the entire pathway can vary from a few coarse divisions to many hundreds of fine divisions. Depending on the mathematical approach, most analyses of Q_{max} have made implicit assumptions about conduit length without explicitly discussing this condition, and they have, in fact, dealt primarily with the theoretical extremes.

(a) *Unitary cavitation response* (n = *1*). Most studies have used this approach, modified only indirectly by the inclusion of other concepts of hydraulic segmentation as discussed above. Jones & Sutherland (1991) emphasized that cavitation was not only expected as a consequence of soil water stress but would also be a direct consequence of a plant's own stomatal behaviour and water-transport processes. Although this was not stated explicitly, these authors dealt with a unitary response as though a single discrete tier of vessels traversed the entire pathway such that $n = 1$. This represents the coarsest partitioning possible, and the entire pathway would then cavitate on the basis of the most negative pressures anywhere in the plant. Use of this system with a linear $f(P)$ (Fig. 2, dotted line; $f(P) = 1 + mP$, where m is the slope of the cavitation response) permits the direct simultaneous solution of Eqns 1 and 4 (see Appendix). The general expression relating the dependence of Q on leaf xylem pressure (P_1) can be used to calculate the partial derivative of Q with

respect to P_1 ($\delta Q/\delta P_1$), and the value of P_1 associated with the maximum possible Q:

$$P_{1@Q\max} = -\frac{1-mP_0}{2m} \qquad \text{Eqn 6}$$

The nomenclature here follows that diagrammed in Fig. 1c (only in this single-tiered case $n = 1$ and $P_n = P_1$), with P_0 representing the pressure equivalent of total water potential in the soil, P_1 the most negative xylem pressure reached at the distal end of the xylem pathway within the plant (generally the leaf), and m the slope of the cavitation response. This expression has some interesting implications, because substituting it back into the simultaneous solution of Eqns 1 and 4 leads directly to (see Appendix):

$$Q_{\max} = K_0\left(\frac{K}{K_0}\right)\Delta P$$

$$= K_0\left(0.5\frac{P_{@K=0}-P_0}{P_{@K=0}}\right)[\tfrac{1}{2}(P_0-P_{@K=0})] \qquad \text{Eqn 7}$$

($Q_{\max}$, the maximum allowable flow for $n = 1$; $P_{@K=0}$, the negative pressure at which cavitation would reach 100%.) This tells us, first of all, that achieving maximum Q necessitates high levels of total conductance loss. This loss would be a constant value of 50% throughout the pathway at $P_0 = 0$, and would be even larger as soil water potential declined. The magnitude of ΔP associated with this 50% conductance loss would be just halfway to that which would cause 100% cavitation.

(b) *Infinitely partitioned response* ($n = \infty$). Sperry *et al.* (1998) recognized that, in most plants, cavitation becomes progressively greater in distal portions in comparison with basal portions of the plant owing to the pressure gradient. They incorporated an integral calculation, matric flux potential (Campbell, 1985), in which each infinitesimally short longitudinal element along the pathway possesses an independent cavitation response to its own pressure. The maximum value of Q under matric flux is:

$$Q^*_{\max} = K_0\int_{P_{@K=0}}^{P_0} f(P)\,\mathrm{d}P \qquad \text{Eqn 8}$$

($Q^*_{\max}$ represents the flow rate that could be achieved if cavitation were completely restricted to the sites of origin.) With regard to Fig. 1c, $Q^*_{\max}$ embodies a contradiction. The cavitation response proceeds as though the pathway were divided into an infinite number of tiers. Clearly if n were infinite, however, pit resistance as defined in Eqn 2 would be infinite and Q would be zero. Eqn 8 thus represents a theoretical endpoint for cavitation dynamics, but K_0 must be assigned an empirical value. Nevertheless, matric flux is an important theoretical reference point and is an excellent computational method when n is large. With the use of the same linear $f(P)$ discussed above for Eqns 6 and 7, Eqn 8 is equivalent to (see Appendix):

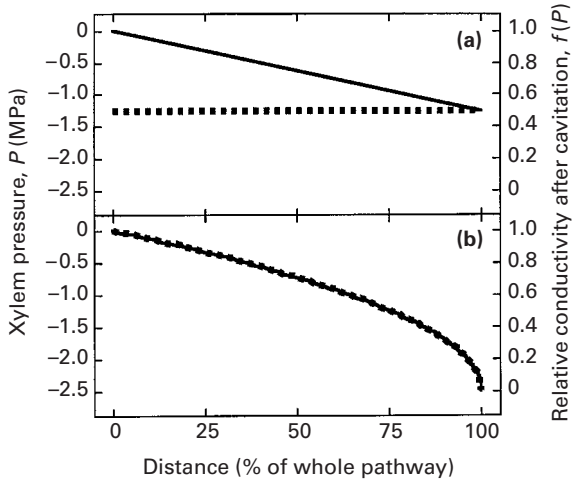

Fig. 3. Gradients of xylem pressure (left-hand y-axis) and fractional conductivity loss from cavitation (right-hand y-axis) associated with two extreme concepts of cavitation containment. In both cases the profiles shown are those that would be present at $Q_{\max}$, but the superior cavitation containment in (b) actually allows a value of $Q_{\max}$ twice as large as that in (a). (a) A unitary response with no cavitation containment. Flux dynamics were modelled in accordance with Eqns 6 and 7. Conductivity in the entire pathway was reduced on the basis of the single lowest pressure at the distal end of the pathway ($n = 1$). (b) A pathway with perfect cavitation containment, in which flow was modelled by using matric flux (Eqn 9), such that each infinitesimal length element had a unique conductivity on the basis of its own xylem pressure only ($n = \infty$). All other aspects of initial conductivity before cavitation, and the cavitation vulnerability, $f(P)$, are identical in (a) and (b). Solid lines, P; dotted lines, $f(P)$.

$$Q^*_{\max} = K_0\left(\frac{K}{K_0}\right)\Delta P$$

$$= K_0\left(0.5\frac{P_{@K=0}-P_0}{P_{@K=0}}\right)(P_0-P_{@K=0}) \qquad \text{Eqn 9}$$

Of interest here is that the middle factor, corresponding to K/K_0, is identical between Eqn 9 and the single-tier model (Eqn 7). This is because $Q_{\max}$ is dependent on the product of $f(P)$ and ΔP, and there is a direct compromise between these two factors. With the simple linear slope used here for $f(P)$, the product is always maximized by sacrificing exactly half of the initial value of K_0 during the development of an optimal ΔP. Of crucial importance is the fact that, with equivalent parameterization of the pathway (i.e. K_0, m and P_0), $Q^*_{\max}$ is twice $Q_{\max}$ calculated for a unitary cavitation response. This difference is entirely attributable to the greater ΔP predicted in Eqn 9 compared with Eqn 7 as explained in the next section.

(c) ΔP *and cavitation containment*. These major differences between the predictions of ΔP for Eqns 7 and 9 can be understood by examining the pathway profiles of P and the remaining conductivity after

cavitation associated with Q_{max} in the two different extremes (Fig. 3a,b). For the single-tiered ($n = 1$) model there is no cavitation containment, and pathway conductance is determined by the most negative pressure in the plant. This results in a conductivity reduction that is uniform throughout the pathway (Fig. 3a, dotted line). Because conductivity and Q are both constant throughout the pathway, the xylem pressure profile is also linear throughout (Fig. 3a, solid line). Total ΔP across the whole pathway cannot be increased further without actually causing a decrease in Q owing to an excessive reduction in conductivity throughout the pathway.

By contrast, the matric flux model ($n = \infty$) assumes that cavitation at each point depends only on P at that point and that there is perfect cavitation containment. In the basal portion of the pathway, P is still close to P_0 and conductivity is initially very high in Fig. 3b. As P becomes more negative moving downstream, the degree of cavitation increases in exact proportion, so that the pressure and conductivity profiles (Fig. 3b, solid and dotted lines, respectively) are superimposed on one another. Although conductivity has a markedly different profile in the two cases, which is consistent with the summary Eqns 7 and 9, the total conductance loss of the entire pathway at Q_{max} is identical. However, because ΔP has twice the magnitude in Fig. 3b, Q^*_{max}, with perfect cavitation containment, is twice as great as Q_{max} for the unitary response with no cavitation containment.

At the extreme end of the flow path in Fig. 3b is a pressure that causes 100% cavitation. This seems like a contradiction, because Q must be constant throughout the pathway – but how can Q be greater than zero when $K/K_0 = 0$? The answer is that this is merely a boundary condition at the end of the flow path, and there is no flow actually passing through that point. The apparent paradox arises only because we are evaluating a limit that defines Q^*_{max}. The benefit of high n lies, then, in the high K maintained in the basal portion of the pathway, and the restriction of cavitation to elements of infinitesimally short length, allowing the very steep final gradient in P at the distal end and the much larger total ΔP over the whole pathway. This results in a higher Q_{max}.

Neither of the theoretical extremes $n = 1$ and $n = \infty$ recognize the real anatomy of the xylem, in which conduit length divides the pathway into many tiers that can partly, but not completely, restrict the spread of damage from the sites of cavitation origin. All real plants therefore lie somewhere between the extreme predictions of Eqns 7 and 9.

IV. INCLUDING VESSEL LENGTH IN A TRANSPORT MODEL

1. *Framing questions of optimal conduit length*

In this section we evaluate maximum transport rates in the xylem when the effects of vessel length are explicitly included in determining both initial resistance and the dynamics of cavitation throughout the pathway. For the intermediate cases of $1 < n < \infty$ it is more difficult to develop analytic solutions such as those already detailed for the extremes. Consequently, we rely extensively in this section on the results of a numerical simulation model to define these effects initially for linear $f(P)$ (Fig. 2, dotted line). We demonstrate that explicit expressions such as Eqns 7 and 9 (but for any n), can, in fact, be derived by inductive logic from these simulation results, and verify that these general expressions are consistent with the analytic solutions for the cases $n = 1$, 2 and ∞. We conclude this section with a discussion of the same processes when the cavitation vulnerability function, $f(P)$, has a more typical, curvilinear shape (Fig. 2, solid line).

We shall ultimately develop an expression for optimal n in terms of a compromise between the positive effects of containment of cavitation, and the negative effects of increased initial resistance. The increased initial resistance is simply modelled as nR_{pit}, but the containment of cavitation has subtler aspects that must be developed in some detail. These questions are made more complex because, once the pathway is divided into two or more tiers, we must concern ourselves not only with the value of n but also with the precise placement of the end walls of each tier at l_1, l_2, …, l_n (Fig. 1c). Although the tiers are shown schematically in Fig. 1c as though they were all of equal length, an examination of Fig. 3b suggests that uniform tier length is unlikely to be an optimal solution. The advantage of partitioning the pathway is in preventing distal water potentials from affecting the conductance in proximal portions of the flow path. If the water potential gradient through the plant is curvilinear, with more rapid changes in the distal regions, then the benefits of partitioning are greater distally, where dP/dl is steeper. We develop this concept explicitly towards a mathematical definition of optimal conduit tier-length distribution (OCLD) before returning to a final analysis of the optimal value for n itself.

2. *A numerical model for flow through* n *conduit tiers*

(a) *Model structure*. We developed a numerical model based on a very simple representation of the flow path (Fig. 1c) that has the following characteristics:

(1) uniform lumen resistivity ($R_{lumen}(l)dl$) throughout its length;

(2) fixed total lumen resistance (before cavitation) and length (L);

(3) uniform vulnerability to loss of hydraulic conductance due to cavitation with decreasing xylem pressure, $f(P)$ (in our initial discussions, we focus exclusively on linear $f(P)$, returning to curvilinear $f(P)$ in a concluding section);

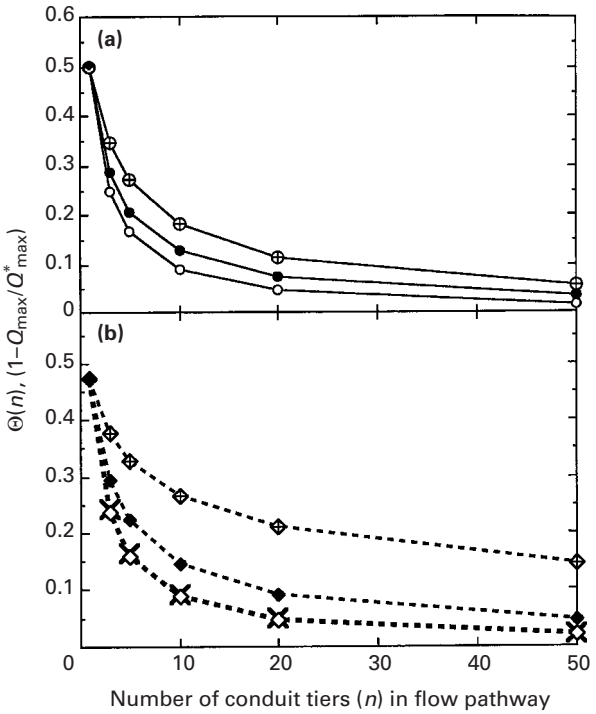

Fig. 4. Θ, the limitation imposed on Q_{max} by the incomplete containment of cavitation at the sites of origin. Θ is a function of both n and the conduit tier-length distribution, $\{l_i\}$, and reflects solely the effects of n on cavitation dynamics while excluding the effects of nR_{pit} (R_{pit} was set to 0). Maximal flow relative to which limitation is defined is an axis with the same K_0 and $f(P)$ but exhibiting cavitation dynamics as though $n = \infty$. This reference flux was calculated by using matric flux potential (Eqn 8). (a) Linear cavitation vulnerability $f(P)$; Θ is calculated for pathways with a range of n from 1 to 50, and with $\{l_i\}$ uniform (closed symbols), optimal (open symbols) or 'inverted-optimal' (symbols containing a + sign) along the axis. (b) Weibull function $f(P)$; uniform-CLD, closed diamonds; OCLD, open diamonds; inverted OCLD, hatched diamonds; linear OCLD, crosses. The latter is a hybrid analysis (Ï) in which actual cavitation follows the Weibull function $f(P)$ but the $\{l_i\}$ of the pathway is that defined as optimal under linear, not Weibull function, $f(P)$ (Eqn 14).

(4) steady-state water flux (Q);

(5) a defined number of conduit tiers with all conduit end walls in common planes and a single conduit length class within each tier.

The concept of solving for water potential gradients and flow rates in a multi-tiered pathway is similar to that discussed above in the single-tiered case: We must solve Eqns 1 and 4 simultaneously:

$$Q = K\Delta P = \frac{1}{\Sigma_{i=1}^{n} R_i}(P_0 - P_n) \qquad \text{Eqn 10}$$

(ΣR_i, the sum of final resistances in each tier after cavitation; $P_0 - P_n$, the total ΔP across all tiers in the pathway.) However, the situation is greatly complicated for the multi-tiered pathway because solving for ΣR_i requires solving for an array of n values of P_i, which determine the different levels of cavitation in each discrete tier. Lacking a direct solution to the array $\{P_i\}$, we determined it by numerical approximation.

Because Q is assumed to be in steady state throughout the pathway, Q must conform not only to Eqn 10 but also to the analogous expressions for each tier individually:

$$Q = \frac{f(P_1)}{R_{0.1}}(P_0 - P_1) = \frac{f(P_2)}{R_{0.2}}(P_1 - P_2)\ldots$$

$$= \frac{f(P_n)}{R_{0.n}}(P_{n-1} - P_n) \qquad \text{Eqn 11}$$

$R_{0.i}$ is calculated, following the schematic in Fig. 1c, as:

$$R_{0.i} = R_{pit} + \int_{l_{(i-1)}}^{l_i} R_{lumen}(l)\ \mathrm{d}l \qquad \text{Eqn 12}$$

(b) *Model solution.* In most applications, we were interested in Q_{max}, the highest possible value of Q consistent with Eqn 10 for a system composed of n conduit tiers. This was done by an iterative search algorithm that first postulated a possible value of Q (Q_{guess}), and then performed simultaneous solutions of Eqns 1 and 4 for each conduit tier sequentially. As shown in Eqn 11, the distal pressure determined for each conduit tier became the proximal pressure of the next tier. The core subroutine thus solved for the array, $\{P_i\}$, needed to evaluate n tier-specific levels of cavitation during transport. Q_{guess} was rejected if any tier failed to have a viable solution. If all tiers could support Q_{guess}, a larger value was tested until Q_{max} was identified. A geometrically decreasing Q_{guess} neighbourhood approach was taken to search for Q_{max}, permitting an estimation precision of 1 in 10^9 after 30 iterations.

3. *Optimization when* f(P) *is linear*

(a) *Isolating the effects of* n *on cavitation containment.* It was useful, for two distinct reasons, to develop an expression defining the effects of n on cavitation containment alone, without regard for the effects of nR_{pit} on R_0. First, nR_{pit} is already incorporated in Eqn 2, and an additional expression for cavitation containment alone will lead us to a quantitative evaluation of the compromise between these two opposing effects of n. This will permit a theoretical analysis of optimal n in a later section. Second, but equally important, most empirical studies of hydraulic architecture determine R_0 directly with measurements that include both lumen and pit resistances at once. In such circumstances, the effects of nR_{pit} are already accounted for, but to model the flow behaviour it is then necessary to know how n affects the cavitation dynamics alone.

This was achieved by running a first set of simulations with R_{pit} set to zero, and allowing only the effects of variable partitioning and cavitation containment. Because absolute transport rates are strongly influenced by nR_{pit} as well, it was most

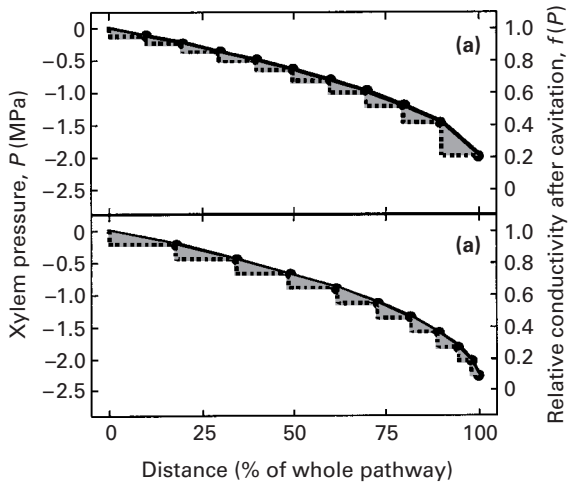

Fig. 5. Xylem pressure and conductivity profiles associated with a multi-tiered cavitation response along a flow path with $n = 10$. All axes are the same as in Fig. 3, with the left-hand y-axis showing the xylem pressure and the right-hand y-axis the relative conductivity, $f(P)$, remaining after cavitation. (a) Uniform tier lengths throughout the pathway ($Q = 0.13$); (b) optimal conduit tier-length distribution (OCLD) as defined by Eqn 14 ($Q = 0.09$). In both panels, flux dynamics were calculated in identical fashions, solving for Q_{max} by using Eqns 10, 11 and 12, with $\{l_i\}$ and its effects on cavitation containment being the only distinguishing features. Q_{max} is slightly higher in (b), as indicated by the lower value of Θ (0.13 and 0.09 for uniform conduit tier-length distribution and OCLD, respectively). Solid lines, P_i; dotted line, $f(P_i)$; circles, conduit endpoints.

appropriate to express these isolated effects on cavitation containment in relative terms. We defined a relative containment limitation (Θ) as the fractional reduction in Q_{max} at a given n relative to perfect containment when $n = \infty$ as:

$$\Theta(n) = 1 - \frac{Q_{max}}{Q^*_{max}} \qquad \text{Eqn 13}$$

$\Theta(n)$ then describes the fractional decrease in Q_{max} at a defined n, related solely to the spread of cavitation away from the sites of origin as a consequence of conduit length. In evaluating Eqn 13, we solved for Q_{max} by using the numerical model recognizing n conduit tiers, and calculating Q^*_{max} with the matric flux potential equation (Eqn 8).

$\Theta(n)$ changes rapidly at low n. A single-tiered pathway, as already discussed, has its Q_{max} reduced by a factor of 0.5 from a lack of cavitation containment. For a linear $f(P)$ and tiers of uniform length (Fig. 4a, solid circles), the containment limitation decreased to < 0.1 by $n = 10$ and to < 0.05 by $n = 50$. The nature of this changing limitation might be understood further by considering the water potential gradient and cavitation profile (at Q_{max}) in a pathway with $n = 10$ and all tiers of equal length (Fig. 5a). Comparing this diagram with Fig. 3a, we see that each individual tier in Fig. 5a had features that were highly reminiscent of the single-tiered pathway. There was uniform cavitation within each tier, and it was determined by the lowest value of P within the tier. The shaded triangular regions in Fig. 5 visually display the tier-by-tier penalty that is paid in lowered conductivity from the lack of cavitation containment within tiers. However, in comparison with Fig. 3a we see that (1) the total effect of uncontained cavitation was much less at the higher n, and (2) at higher n the pathway could sustain a greater total decrease in water potential across it at Q_{max}.

This latter point of higher total ΔP merits special emphasis. Recall that in comparing the single-tiered and matric-flux models, the percentage loss of hydraulic conductance in the two conditions was the same at Q_{max}, and differences in Q_{max} were attributable entirely to differences in ΔP. The same principle holds for multi-tiered pathways at intermediate n. Containment of cavitation by greater partitioning reduces conductance loss substantially. At submaximal Q, this effect would be quite evident in comparisons of K. However, when all example systems have been driven to their respective maxima for Q, variation in K tends to disappear. These maxima will all depend on the product of K and ΔP, and, regardless of the rate in decline of K with total ΔP at different values of n, the maximum always occurred at a predictable percentage decrease in K_0. On the basis of a linear $f(P)$, this was exactly 50% for the single-tiered and matric-flux pathways (Eqns 7 and 9). For a multi-tiered pathway with $n = 10$, it was close to 50% for tiers of uniform length, and exactly 50% if the tier length was distributed optimally with respect to cavitation containment as discussed in the next section.

(b) *Optimal conduit tier-length distributions* (*OCLDs*). We expect the containment of cavitation to be sensitive, not just to the value of n but also to the subtler aspects of the mean lengths of conduits in different parts of the pathway. This is expected to arise from the steeper $\partial P/\partial l$ in distal portions of the pathway, and the rapidly increasing levels of cavitation associated with it. Although we might expect that the optimal frequency of end walls increases distally in the shoot, it is not obvious a priori how different from each other the basal and distal regions should actually be. To explore this question numerically, we added a second, nested search algorithm to the simulations of Q_{max}. The new algorithm optimized the partitioning of initial resistance into n compartments by varying the set of end-wall positions $\{l_i\}$ (Fig. 1c). The total length and resistance of the pathway as a whole were held constant, but the integrals of $R_{lumen}(l)$ representing each individual tier (Fig. 1c; Eqn 12) were allowed to exchange lengths while searching for an optimal set of $\{l_i\}$. Optimization was based on the $\{l_i\}$ value that yielded the highest Q_{max}.

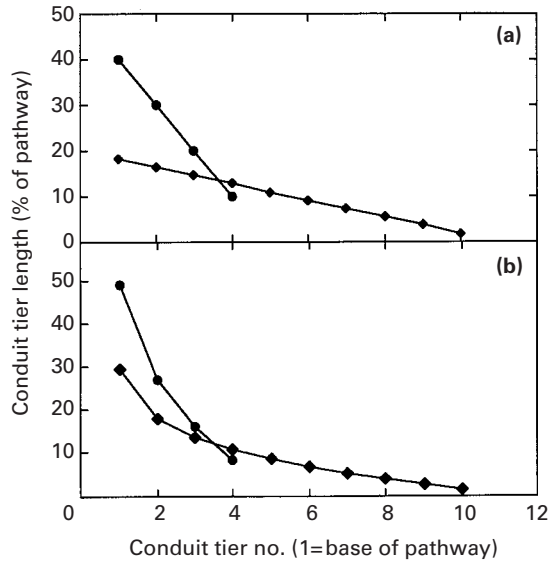

Fig. 6. The optimal conduit tier-length distribution (OCLD) shown as relative tier length against tier position. The OCLD is shown for different numbers of conduit tiers; $n = 4$ (circles) and $n = 10$ (diamonds). At OCLD the system reaches its greatest possible Q_{max}. (a) OCLD for linear cavitation vulnerability function, $f(P)$; (b) OCLD for Weibull function, $f(P)$.

In Fig. 6a the results are shown for two cases, with $n = 4$ and 10, respectively. Two features are immediately obvious: the optimal length of the conduit tiers decreased substantially between the basal and distal ends of the pathway, and it did so in a continuous fashion. A generalized expression predicting the OCLD for any n was:

$$\frac{L_i}{L} = \frac{(n+1)}{\Sigma_1^n i} - \frac{i}{\Sigma_1^n i} \qquad \text{Eqn 14}$$

($L_i = l_i - l_{(i-1)}$; it represents the total length of the ith tier.) This expression is not particularly intuitive at first glance, but it is simply a linear function of i, the rank position of a given tier in the pathway as shown in Fig. 6a, with both slope and intercept given as functions of n to make it general. Thus, Eqn 14 predicted both the OCLD shown for $n = 4$ and $n = 10$, and likewise for any n. A pathway with the spacing of the end walls distributed according to Eqn 14 contained the effects of cavitation more effectively near the sites of origin than any other possible length distribution still with the same n (this is proved analytically for the case of $n = 2$ in the Appendix).

A comparison of $\Theta(n)$ between OCLDs and uniform tier lengths is given in Fig. 4a (open circles compared with closed circles, respectively). At very high values of n, containment became quite effective for both OCLD and uniform tier-length distributions. At moderate values of n, however, the superiority of the OCLD was substantial. At $n = 10$, for example, shifting from uniform tiers to OCLD was as effective at reducing Θ as doubling n. In terms of adaptive response, adopting an OCLD does not carry any penalty in terms of increased nR_{pit}, as would increasing the value of n (see section IV.3.d). A reversal of the pattern of OCLD, with mean conduit length increasing from basal to distal regions, would be particularly maladaptive (Fig. 4a, circles with + superimposed).

Fortunately, for a pathway with linear $f(P)$ and an OCLD, the laborious computations of numerical simulation for evaluating $\Theta(n)$ are unnecessary. The exact magnitude of the cavitation containment limitation could be predicted by a simple algorithm for any value of n (see Appendix):

$$\Theta(n) = 1 - \frac{n}{n+1} \qquad \text{Eqn 15}$$

Further, at OCLD, the loss of whole-pathway conductance at Q_{max} was 50% for all n. Therefore, the containment limitation was solely a function of how ΔP changed with n rather than an effect of pathway conductance.

(c) *Abrupt changes in conduit length.* Eqn 14 predicts that, in OCLD, changes in length, or at least in the partitioning of resistance between tiers, should be gradual and continuous from the basal to distal regions. Under catastrophic conditions in which Q_{max} might be exceeded, the collapse of the transport system would occur initially in a single critical tier. For most length distributions, the terminal, distal tier, where P was lowest and cavitation was greatest, was also the tier in danger of immediate hydraulic failure. Basal portions of the pathway were generally under very little stress, whereas the limitation to overall flow was set by the most distal tier, where cavitation levels were high. However, such a bottleneck effect is not theoretically restricted to the final tier under non-OCLD. A bottleneck can theoretically occur at intermediate tiers if the conduit length undergoes an abrupt rather than a gradual shortening, such that very long conduits have their ends near the distal end of the entire flow path where P is most negative. This kind of abrupt shortening might occur, for example, in the twig or petiole of a ring-porous tree or vine, and this could shift the critical conduit tier in immediate danger of collapse to the last very long tier of conduits in the pathway (i.e. the twig or branch). In such length distributions, the location within the pathway of incipient hydraulic failure at Q_{max} depends both on the tier-length distribution and interactions with hydraulic segmentation represented by variation in $R_{lumen}(l)$, as discussed in more detail in section V.3.a.

(d) *Optimal frequency of end walls: incorporating* R_{pit}. The optimal value of n, n_{Qmax}, was defined as that which permitted the highest possible value of Q, $Q_{max}^{n=opt}$. Considering Fig. 4a alone, the optimal n would be ∞, because this resulted in the minimum containment limitation. However, in a complete analysis of the effects of n, the gain of greater

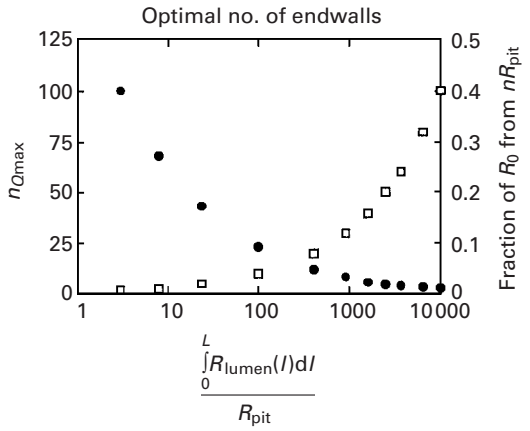

Fig. 7. Optimal number of end walls ($n_{Q\max}$ (open squares); left-hand *y*-axis) achieving the greatest possible $Q^n_{\max}$ based on a compromise between pit membrane resistance vs cavitation containment. High n favours increased cavitation containment (Fig. 4) but causes higher initial flow resistance (K_0, Eqn 2). $n_{Q\max}$ (Eqn 17) is a function of the ratio of whole-pathway lumen resistance to pit resistance (*x*-axis). Also shown (closed circles) is the contribution of total pathway pit-membrane resistance (nR_{pit}) to R_0 (right-hand *y*-axis).

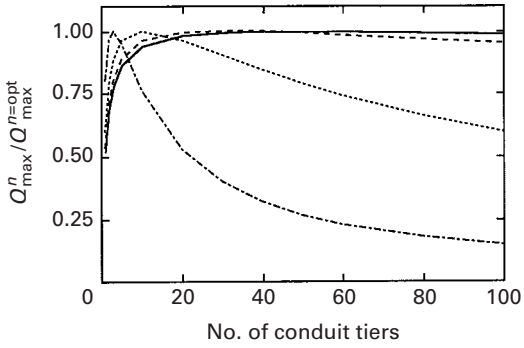

Fig. 8. The sensitivity of $Q_{\max}$ to deviation of n from $n_{Q\max}$. Curves for different values of $n_{Q\max}$ (dot-dashed, $n_{Q\max} = 3$; dotted, $n_{Q\max} = 10$; broken, $n_{Q\max} = 20$; solid, $n_{Q\max} = 50$) are based on different values of R_{pit} whilst holding $\int R_{lumen}(l)dl$ constant in all analyses. The *y*-axis is plotted as a relative value to emphasize curve shape and the contribution of n rather than the different values of R_{pit} in controlling $Q_{\max}$.

cavitation containment as n increases would be offset by higher nR_{pit} in the determination of K_0 (Eqn 2). This compromise should lead to an intermediate, optimal value of n, depending on the relative values of R_{pit} and $R_{lumen}(l)$. Although $R_{lumen}(l)$ can be readily estimated from the Hagen–Poiseuille equation (Eqn 3), there is relatively little information on R_{pit} beyond the tracheid analysis of Nobel, Gibson and colleagues in which nR_{pit} can reach a magnitude equal to $\int R_{lumen}(l)dl$ (Gibson *et al.*, 1984; Calkin *et al.*, 1986; Schulte & Gibson, 1987; Veres, 1990). In the optimization analysis that follows, it was assumed that cavitation caused equal reductions in lumen and interconduit pit components of total pathway conductance.

Defining an analytical expression for the optimal number of end walls subdividing the pathway into multiple tiers begins with Eqns 7 and 9. First, we substituted into Eqn 2 for K_0. Second, we concluded that the middle factor, describing K/K_0 after cavitation at $Q_{\max}$, would be constant for all n as already discussed and in the Appendix. Finally, we drew upon Eqn 15 and our conclusion that the cavitation containment limitation was fully described by a factor of $n/(n+1)$, which quantifies how sustainable, total ΔP varies with n. This yields:

$$Q^n_{\max} = \left[\frac{1}{nR_{pit} + \int_0^L R_{lumen}(l)\,dl}\right]\left[0.5\frac{(P_{K=0} - P_0)}{P_{K=0}}\right] \times \left[(P_0 - P_{K=0})\frac{n}{n+1}\right] \quad \text{Eqn 16}$$

In this expression, $Q^n_{\max}$ refers a family of pathways differing in n but always possessing an OCLD. The added superscipted n is present to emphasize that we are looking for a global maximum in Q with respect to optimization of the xylem anatomy, and not just a specific maximum under an arbitrarily fixed anatomical definition. To find the unique value of n yielding the highest possible value for $Q^n_{\max}$, we took the partial derivative $\partial Q^n_{\max}/\partial n$, set it equal to zero and solved for of $n_{Q\max}$:

$$n_{Q\max} = \sqrt{\frac{\int_o^{l_n} R_{lumen}(l)\,dl}{R_{pit}}} \quad \text{Eqn 17}$$

All effects of P_0 cancelled out of Eqn 17, indicating that, for linear $f(P) = 1 + mP$, the solution was generally valid regardless of what combination of high flux and/or low soil water potential was causing the pathway to reach its transport limit.

Eqn 17 yielded the simple result that the optimal number of conduit tiers was related to the ratio of the integrated lumen resistance of the entire pathway to the resistance of crossing the pit membranes of a single tier of conduits. As shown in Fig. 7 (left-hand *y*-axis), the smaller the pit resistance there was relative to the pathway lumen resistance, the higher $n_{Q\max}$ was. Intuitively this is logical, given that when we set $R_{pit} = 0$ and remove any hydraulic cost of pit resistance, $n_{Q\max} = \infty$ (Fig. 4a). Conversely, the more hydraulic resistance there is at the pits, the lower $n_{Q\max}$ is. The right-hand *y*-axis in Fig. 7 shows the implied contributions of nR_{pit} to total K_0, as implied by the ratio $\int R_{lumen}(l)dl/R_{pit}$ (*x*-axis) combined with the respective values of $n_{Q\max}$ (left-hand *y*-axis). This was included for ease of comparison of the optimality predictions with published values, although in fact there are currently few data sets in which this is confidently evaluated (see section V.2.a). Fig. 8 shows how the $n_{Q\max}$ optimum became progressively flatter as $n_{Q\max}$ increased. This was because, at high values of $n_{Q\max}$, both of the opposing effects were changing only very slowly with n. The asymptotic nature of the cavitation limitation at high n is evident in Fig. 4, and high $n_{Q\max}$ in Figs 7 and 8

was associated with very low R_{pit}, such that large changes in n were needed to change K_0 substantially.

4. *Optimization when* f(P) *is curvilinear*

All discussion so far has centred on an assumed linear $f(P)$ of the form shown in Fig. 2. This has helped us to derive relatively simple expressions and conclusions, but real plants often have much more complex shapes to their cavitation vulnerability curves. There is no theoretical reason to expect a specific shape for $f(P)$ other than that it must be a monotonically decreasing function, and several functional types have been used to fit data empirically on curvilinear vulnerability (Sperry & Tyree, 1990; Neufeld *et al*., 1992; Mencuccini & Comstock, 1997; Sparks & Black, 1999). One useful formulation is the Weibull function (Fig. 2, solid line), first applied to vulnerability curves by Neufeld *et al*. (1992). The use of a Weibull function to define $f(P)$ in our analysis gave results that were qualitatively very similar to the linear case in almost all important respects, although concise analytic expressions for general relationships, such as Eqns 14, 15 and 17, could not be derived with the same precision.

The OCLD determined for the Weibull function by our numerical search algorithm is shown in Fig. 6b. The OCLD was in some respects very similar to that predicted for linear $f(P)$, in that basal segments were much longer than distal ones, and the transition was graded, not abrupt. However, there were notable differences as well. The rate of change was curvilinear, and the difference between basal and distal tiers was even more extreme. More significantly, the predicted OCLD was not independent of P_0 (not shown), as it was with linear $f(P)$. Obviously, a plant cannot change the dimensions of pre-existing, no longer living, xylem conduits in response to a change in soil water potential, so we must ask how quantitatively important these effects were.

The containment limitation $\Theta(n)$ showed qualitatively similar patterns to those already discussed, but a pathway with Weibull function $f(P)$ was even more sensitive to tier-length distributions than the same analyses when $f(P)$ was linear (Fig. 4b). When each curve type was at its own respective OCLD, there was remarkable congruency of $\Theta(n)$ between Weibull and linear cases (Fig. 4, open diamonds in Fig. 4b compared with open circles in Fig. 4a, respectively). This means that Eqn 15, although precisely correct only for linear $f(P)$, was still an excellent approximation for the Weibull function $f(P)$. Moreover, changing the length distribution, $\{l_i\}$, of the Weibull function from its own numerically determined optimum to that defined by Eqn 14 for linear $f(P)$ made an almost imperceptible change in $\Theta(n)$ (Fig. 4b, open diamonds compared with $\times$ symbols). Eqn 18 for $n_{Q\max}$ was also an almost perfect approximation for the Weibull function when $P_0 = 0$, but the disparity could be 15–20% if P_0 were low enough to cause very high levels of cavitation (50%) even in the absence of water transport. However, it should be noted how flat the optima were for $n_{Q\max}$ in Fig. 8, so even here the differences in predicted $Q_{\max}^{n=\text{opt}}$ were very small.

V. CONDUIT LENGTH IN MODERN TAXA: IMPLICATIONS FOR TRANSPORT

1. *Limitations to the concept of conduit tiers*

(a) *Vessel ends are randomly distributed*. Evaluating n for real plants involves consideration of their much more complex conduit length distributions. Conduits are rarely organized into distinct tiers, and multiple length classes coexist throughout the pathway. The assumption of discrete tiers in the models already discussed was a conceptual and computational aid. However, this simplification has little effect on the general conclusions. Having conduit ends randomly scattered along the axis rather than organized into discrete tiers will smooth the apparent step function for k (e.g. Fig. 5) but will not in any way alleviate the inherently greater loss of total conductance resulting from cavitation in longer conduits. Cavitation would still be determined by the most negative water potential at the distal end of each conduit, and would still reduce conductivity in the pathway throughout the conduit's length.

(b) *Dispersion around mean length within each tier*. The consequence of multiple length classes coexisting in all regions of the pathway of real plants is more difficult to evaluate. Having dispersion around the mean conduit length does nothing to alleviate the need for cavitation containment, but the effective value of n, in the context developed here, becomes a complex average of different length classes weighted by their contribution to total K_0. When diameter classes in a xylem cross section are measured, variation in expected flow capacity typically ranges one or two orders of magnitude between different vessels. The smallest half or more of the size distribution typically makes only a minor contribution to K_0 (Ellmore & Ewers, 1986; Ewers & Fisher, 1989a; Sperry *et al*., 1994; Mencuccini & Comstock, 1997). Length classes, generally measured separately from conduit radii, can vary from a few centimetres to several metres, with the short vessels being typically much more numerous (Zimmermann, 1983). It is then essential to know whether the long vessels are also those with greater diameter, so that they dominate K_0 despite being fewer in number. In comparisons between early and late wood, and between different species, there is a consistent and strong positive correlation between length and diameter (Zimmermann & Potter, 1982).

Although reinforcing the same correlation, accurate data on length and diameter size classes for vessels mixed in the same complex tissue are extremely rare (Buchmueller, 1986; Ewers & Fisher, 1989b). A more accurate appraisal of n in most plants awaits the development of techniques making this evaluation tractable, but it is likely that Q_{max} is strongly dependent on the behaviour of the longest and widest vessels, and is thereby potentially limited by the poor cavitation containment in long vessels.

An interesting aspect of these length and diameter distributions within individual stem segments is found in several studies that have shown that, as cavitation decreases K within a given axis, it is the largest vessels in the population that tend to fail first at moderate P (Lo Gullo & Salleo, 1993; Hargrave *et al.*, 1994; Sperry & Saliendra, 1994; Lo Gullo *et al.*, 1995; Linton *et al.*, 1998). At very negative pressures, the population of vessels remaining is often strongly skewed towards the small end of the original size distribution. This would suggest that the initial Q_{max}, when P_0 is high, might be primarily dependent on a subpopulation of the largest vessels, minimizing nR_{pit} and maximizing conductivity via a large diameter lumen. As P_0 decreases under stress, there would be a natural shift to a 'safer' system of shorter, narrower vessels, no longer capable of high flux rates but also no longer susceptible to abrupt failure via cavitation spread from distal regions.

2. *Is the xylem optimally partitioned?*

(a) *Optimal number of end walls.* Analysis of n_{Qmax} indicates that the large numbers of conduit tiers, as seen in many plants, would maximize Q only for values of R_{pit} that result in very small estimates of total pit resistance (Fig. 7). Unfortunately, relatively little is known about the magnitude of total pit resistance in plants. The most comprehensive study was done on fern tracheid pathways, in which as much as 50% of total hydraulic resistance could lie in the interconduit pits (Calkin *et al.*, 1986; Schulte & Gibson, 1987). From Fig. 7, such a large fraction of R_0 coming from R_{pit} would be associated with an n_{Qmax} approaching 1, and these fern pathways, with $n \gg 100$, are clearly not in accordance with this prediction of optimality. This is not entirely surprising, because vessels are thought to have evolved to overcome the developmental constraints limiting optimality in xylem pathways made of tracheids. An alternative solution to increased length is to reduce the pit membrane resistance greatly, which might have happened in the highly specialized torus–margo structure of conifer pits. However, the actual partitioning of resistance between lumen and pit in conifers is not known and we cannot yet judge how close they might lie to the predictions of n_{Qmax}.

The evolution of vessels surely brought plants closer to n_{Qmax}, because the much longer conduits allow a range of n from perhaps a few hundred in diffuse porous trees to as low as 10 or 20 in some herbs, vines and trees with very large vessels. However, here, too, precise evaluation is limited, not only by the need for better evaluation of n itself, as discussed above, but also by the absence of definitive data on pit resistance. In some plants with very long vessels, the K_0 of the xylem approaches that predicted by the Hagen–Poiseuille equation for the lumen alone (Eqn 3) (Ewers *et al.*, 1990), but more commonly ranges from only 30% to 95% of this value (Chiu & Ewers, 1992). This lower value of K_0 could indicate substantial additional resistance from the interconduit pits (Zimmermann & Brown, 1971). However, when the measured K is less than that predicted from Hagen–Poiseuille, it is hard to tell whether this is due to a large percentage of R_0 coming from nR_{pit} (Eqn 2) or from the sensitivity of the $R_{lumen}(l)$ estimate to accurate measurement of hydraulic radius (Calkin *et al.*, 1986; Tyree & Ewers, 1991). The estimation of nR_{pit} by subtraction of Eqn 3 from measured R_0 also assumes that the typical wide range of diameters measured from a single xylem tissue cross section represents a population of cylindical conduits that genuinely have different diameters throughout their lengths. If they actually represent conduits cut at different points along similar tapered lengths (i.e. the variation is due to the position of cut only), then the large and small diameters are really in series, not in parallel, and the expected conductivity of the tissue will be much lower. Comparison of specific conductivities of branch segments both shorter than and longer than the average vessel length has sometimes supported the idea that pit resistance makes a very small contribution to the total (Chiu & Ewers, 1993), and this would predict a large value for n_{Qmax} in Eqn 17. Despite this considerable ambiguity, it seems likely that plants with rather small numbers of vessel tiers, such as vines, ring-porous trees or short-statured herbaceous plants, are closest to n_{Qmax}, whereas short-vesseled diffuse-porous trees are more likely to exceed it.

In this context it is worth noting that, owing to the broad n_{Qmax} optima (for $n_{Qmax} > 20$; Fig. 8), n_{Qmax} could be exceeded substantially without a substantial diminution in Q_{max}. Advantages of $n > n_{Qmax}$ might lie in increased safety from mechanical injury, morphological or developmental constraints, susceptibility to cavitation from freezing, and/or other influences not considered here.

(b) *Conduit length distribution along the pathway.* Some clear anatomical patterns in the published papers are consistent with theoretical predictions of substantial decreases in conduit length towards the downstream end of the flow path. According to the OCLDs of Fig. 6, the upstream portion of the flow path (roots) should have substantially longer mean

vessel lengths than downstream ones, and the transition should be gradual rather than abrupt. Again, published length data are scanty, but roots have consistently larger-diameter vessels than shoots (Grew, 1682; Baas, 1982, 1986; Ewers *et al.*, 1997), and, in the few cases tested, this was also associated with much longer vessels in the root (Zimmermann & Potter, 1982; Kolb & Sperry, 1999a). Where it has been measured, vessel lengths in the shoot are shorter on average than in the larger roots, and conduit length in petioles and twigs can be much shorter than in the main branches and trunks (Salleo *et al.*, 1985).

3. *Hydraulic segmentation*

(a) *Segmentation in hydraulic resistance*. Hydraulic segmentation as described by many authors (Zimmermann & Brown, 1971; Salleo & Lo Gullo, 1983; Zimmermann, 1983; Ewers & Zimmerman, 1984; Salleo, 1984; Sperry, 1986; Sellin, 1988; Lo Gullo, 1989; Cochard *et al.*, 1992; Meinzer *et al.*, 1992; Yang & Tyree, 1994; Joyce & Steiner, 1995; Aloni *et al.*, 1997) is distinct from, but fully compatible with, the concepts developed in this review. We predict that conduit length should divide the total resistance, not length in itself, into an optimal number of tiers to contain cavitation (see section VII.2, Eqn A.6, and section VII.5). Segmentation in resistance can be accounted for in $R_{\mathrm{lumen}}(l)$, and thereby included directly in analyses of optimal partitioning.

An interesting special case arises in vines and ring-porous trees, and perhaps in herbaceous species, where relatively long stem vessels potentially approach the leaf bases, where there can be an abrupt change to shorter vessels. As mentioned in section III.3.c, we found that, when $R_{\mathrm{lumen}}(l)$ was constant, the extension of long conduits to near the end of the flow path could result in hydraulic failure occurring first in the stem rather than in the leaves at the distal end of the flow path. This predicted point of failure would contrast sharply with the prediction that segmentation due to variable $R_{\mathrm{lumen}}(l)$ (Tyree & Ewers, 1991) or $f(P)$ (Tyree *et al.*, 1993) protects the main axes. In the segmentation hypothesis, $R_{\mathrm{lumen}}(l)$ is not constant, and increased $R_{\mathrm{lumen}}(l)$ is typically associated with abruptly smaller-diameter and shorter vessels in small twigs and petioles. It has been interpreted to restrict hydraulic failure to expendable organs by manipulating the site with the steepest pressure gradient. The segmentation hypothesis predicts designed failure in the petiole as an adaptive design protecting the xylem pathway in major branches. A sudden increase in $R_{\mathrm{lumen}}(l)$ would also shift the prediction of failure from branch to petiole in our analyses here. The potential vulnerability of the last long conduits adjacent to an abrupt transition in length actually highlights the need for 'segmentation' in $R_{\mathrm{lumen}}(l)$, to control the sites of hydraulic failure in ring-porous species and other species with vessels that are long relative to their stature.

(b) *Segmentation in cavitation vulnerability*. Vulnerability to cavitation, $f(P)$, can also vary, not just between plants, but among organs within a plant (Tyree *et al.*, 1993; Sperry & Saliendra, 1994; Tsuda & Tyree, 1997; Linton *et al.*, 1998). Incorporating this variation in our model could result in pressure and conductivity profiles considerably more complex than those shown in Fig. 3. Here we comment on only one such model: that in which root systems might be more vulnerable to cavitation than the shoots. Several studies have reported such patterns, and many have also found that within the root system the smaller roots are the more vulnerable (Mencuccini & Comstock, 1997; Sperry & Ikeda, 1997; Sperry *et al.*, 1998b; Kolb & Sperry, 1999a; Linton & Nobel, 1999; Hacke *et al.*, 2000). Some studies have also offered analyses of where the limiting bottleneck defining Q_{max} would occur: (1) in the foliage, where P was lowest, or (2) in the root, where cavitation was more sensitive to P. The results can depend on the soil water potential (P_0): when P_0 is high, failure occurs in the shoot, but when P_0 drops during soil drought, failure shifts to the root system (Kolb & Sperry, 1999a). Where small and large roots are distinguished, failure under drought is localized to the more vulnerable small roots (Hacke *et al.*, 2000).

How should such pathways be partitioned optimally to limit cavitation? The shortest conduits should be found where the possibility of cavitation is greatest, so as to contain the loss of conductivity more effectively. In our analysis in which $f(P)$ is constant along the flow path, cavitation occurs at the downstream end of the pathway, and hence this is where the shortest conduits should be found (Figs 3 and 6). If high cavitation zones are also possible in the smaller roots during drought (Hacke *et al.*, 2000), there should also be short conduits at this upstream end of the flow path. The interior pathways of large transporting roots and main stems seem from most studies to have larger safety margins from cavitation, and would be expected to have the longest conduits. The precise pattern of predicted length distribution would involve a complex interaction of segmentation in $R_{\mathrm{lumen}}(l)$ and $f(P)$, and would need to be modelled for each case. The actual length distributions along the pathway would also need to be measured for comparison with predicted results because no conduit length data exist at this level of resolution.

VI. CONCLUSIONS

1. *Anatomy*

Detailed comparisons of conduit length distribution

along the xylem flow path are lacking, but the general trend indicates that mean conduit length decreases towards the downstream end. This is consistent with maximizing flow capacity by limiting the damage from cavitation at distal regions of the shoot. Mean conduit length throughout the plant body is almost certainly less than that predicted to maximize flow capacity for tracheid-bearing species owing to developmental constraints on conduit length. Although the evolution of vessels has probably brought angiosperms closer to the optimal conduit length distribution, a more precise evaluation requires better knowledge of length distributions and pit membrane resistances (e.g. Fig. 7). Given that there might be a rather flat optimum (Fig. 8), selection against shorter-than-optimal vessels on the basis of cavitation containment vs flow resistance might be offset by additional factors that we have not modelled.

2. *Modelling flow*

Accurate modelling of Q in xylem requires some knowledge of the conduit anatomy: (1) the frequency of true end walls subdividing the pathway's cavitation response and (2) the variation in conduit length in basal vs distal portions of the pathway. For plants with only tracheids, such as conifers, or for many diffuse porous angiosperm trees with relatively narrow and short vessels, n is much greater than 100 and the actual limitation imposed on $Q_{\max}$ by failure to localize individual cavitation events will be at most 2% or 3% (Zimmermann *et al.*, 1982; Zimmermann, 1983; Ewers & Fisher, 1989a; Tognetti & Borghetti, 1994; Hacke & Sauter, 1995; Ranasinghe & Milburn, 1995; Zotz *et al.*, 1997). Flow characteristics in such plants can be accurately and much more simply modelled with the matric flux approach (Eqn 8) (Sperry *et al.*, 1998). However, for many other angiosperms, such as some herbs, lianas, ring-porous trees and tropical trees with large vessel diameters, limitations of 5–15% or more are likely, and might need to be taken into account (Zimmermann & Jeje, 1981; Zimmermann, 1983; Legge, 1985; Neufeld *et al.*, 1992; Fisher & Ewers, 1995). If n is known, $Q_{\max}$ can be effectively modelled in such plants as the product of Eqn 8 and the factor $n/(n+1)$ from Eqn 15. Precise modelling of Q under submaximal conditions might require explicit consideration of conduit length in the cavitation process.

VII. APPENDIX: ANALYTICAL SOLUTIONS AND PROOFS

1. *Analytic solution for* Q_{max} *with a single tier*

Several general-case formulas, presented in section IV, were first developed from inductive reasoning after analysis of extensive output from a numerical simulation model. These include Eqn 14 for OCLD, the optimal $\{l_i\}$ under linear $f(P)$, Eqn 15 describing the cavitation containment limitation, and Eqn 17 defining the optimal number of conduit tiers in the flow path. Although full formal proof of the general case is not tractable for these equations, considerable validation is possible. The first level of proof is that the general expressions always hold when tested under numerical simulation, even for previously unexamined values of n, and that no combination of parameters (i.e. tier-length partitioning and final water-potential gradient through the axis) was found that proved superior (i.e. capable of generating a higher $Q_{\max}$) to the predicted values. Here we present another level of more formal proof that is completely independent of the numerical approximation techniques of our modelling. We consider the analytical solutions to the simplest cases, first $n = 1$ and then $n = 2$, and show that these formal proofs lead precisely to the same special-case expressions predicted by our general equations for all n, and that analysis of the derivatives demonstrates that they are true maxima in these cases. The general expressions developed here are also consistent with matric flux calculations at $n = \infty$.

All discussions below are developed for a linear $f(P)$ cavitation function. All nomenclature follows that in Fig. 1c, but the pathway terminates at P_1 or P_2 for the single-tiered and two-tiered cases, respectively. The single-tiered case is quite simple, and was first presented as an analytical solution in Jones & Sutherland (1991).

We first solve Eqns 1 and 4 simultaneously, giving:

$$Q = \frac{1}{R_{0.1}}(1+mP_1)(P_0-P_1) \qquad \text{Eqn A1}$$

We take the derivative of Q with respect to P_1:

$$\frac{dQ}{dP} = \frac{1}{R_{0.1}}(1+mP_0-2mP_1) \qquad \text{Eqn A2}$$

We set this equal to 0, yielding Eqn 6 from Section III.2.a:

$$P_1 = -\frac{1-mP_0}{2m} \qquad \text{Eqn 6}$$

The second derivative of Eqn A1 is negative at this value of P_1, indicating that this total water potential gradient through the plant, P_0-P_1 as defined by Eqn 6, yields the maximum possible Q.

It is also worth considering what level of conductance loss from cavitation is implied by Eqn 6. We substitute the expression for P_1 from Eqn 6 into the $f(P)$ function to get:

$$\frac{K}{K_0} = 1-m\left(\frac{1-mP_0}{2m}\right) = 0.5(1+mP_0) \qquad \text{Eqn A3}$$

If P_0 is zero, and consequently all cavitation in the plant is caused solely by the gradient driving water movement, the maximum flux is achieved by developing a total ΔP that results in exactly 50% loss of the saturated conductance. We can further rearrange this expression as:

$$\frac{K}{K_0} = 0.5\left(\frac{m^{-1}+P_0}{m^{-1}}\right) \qquad \text{Eqn A4}$$

Since $-1/m$ is the value of P at which cavitation reaches 100% (i.e. $P_{@K=0}$), Eqn A4 makes clear that this 50% loss rule extends in modified form to all soil water potentials. The magnitude of ΔP that is possible declines with soil water potential; at negative values of P_0 considerable cavitation might already have occurred without achieving any water movement. However, Q is always maximized under prevailing environmental constraints when exactly half of the remaining conductance available at $Q = 0$ is further lost to cavitation owing to pressure gradients associated with the plant's own water transport process.

2. *The general case for* n *tiers*

We now assert from inductive analysis of model output at many values of n that, for pathways with an OCLD, (*1*) *Eqn A4 is true for all pathways regardless of* n, *and* (*2*) *Eqn* 6 *is a special case of a general equation also true for all* n:

$$P_n = -\frac{n-mP_0}{(n+1)m} \qquad \text{Eqn A5a}$$

It turns out that it is a special feature of pathways with linear $f(P)$ and OCLD that, at $Q_{\max}$, all ΔP_i are equal (Fig. 5b). Consequently, an even more general form of this expression that defines the set of $\{P_i\}$ at limiting Q for this special case is:

$$P_i = -\frac{i-mP_0}{(n+1)m} \qquad \text{Eqn A5b}$$

These assertions are only strictly true if the pathway has an OCLD, and consequently we must solve for $\{P_i\}$ and $\{l_i\}$ simultaneously. Again, from inductive analysis of simulation output, we found that tier length should decrease in a strictly linear fashion moving from basal to distal portions of the pathway. As discussed in section IV.3.b (Fig. 6 and Eqn 14), this solution was for a rather restrictive case, one in which interconduit pits had no resistance and $R_{\text{lumen}}(l)$, the total lumen resistivity of a pathway cross section, was constant throughout the pathway length. *The same inductive reasoning while allowing* $R_{\text{lumen}}(l)$ *to vary as required for hydraulic segmentation and including realistic values of* R_{pit} *leads to a more general expression predicting OCLD for all* n:

$$\frac{R_{0.i}}{R_0} = \frac{2}{n}\left(1-\frac{i}{n+1}\right) \qquad \text{Eqn A6}$$

This expression says that it is not length in itself that is being optimally partitioned, but rather the total resistance of the pathway regardless of its source. We return to the implications of this below after validating Eqn A6 in the analytic proof for $n = 2$.

3. *Analytic solution for* Q_{max} *with two tiers*

We can further support our general expressions with an analytic solution derived for $n = 2$. Although this is admittedly a small value for n, it includes all of the essential features found in all cases of $n > 1$, including (1) the need to find an optimal partitioning of R_0 in Eqn A6, and (2) cavitation dynamics proceeding to different states in different parts of the pathway. The approach is very similar to that developed above for $n = 1$, except that we are trying to solve simultaneously for both OCLD and ΔP to maximize Q. The actual algebra turns out to be rather formidable, even for $n = 2$, so we resorted to using the program Mathematica to calculate the derivatives. Here we only set up the initial equations and then report the analytic solutions found.

First, we define a partitioning variable (a) describing what fraction of the total pathway resistance should be included in the first tier, with fraction $(1-a)$ remaining for the second, final tier of conduits. We then write that:

$$Q = \frac{1}{R}(P_0-P_2) = \frac{1}{R_1+R_2}(P_0-P_2)$$

$$= \frac{1}{R_0\{[a/f(P_1)]+(1-a)/f(P_2)\}}(P_0-P_2) \qquad \text{Eqn A7}$$

This expression is analogous to Eqn A1 for the single-tiered case, except that it includes our partitioning variable and separate cavitation responses in each tier. However, we wish to take two partial derivatives, $\partial Q/\partial a$ and $\partial Q/\partial P_2$, and Eqn A7 is still complicated by being a function of two plant water potentials, P_1 and P_2, not just P_2. We can address this by recognizing that, although they have different values, P_1 and P_2 cannot vary independently. The value of P_1 can be constrained by recognizing that Q is a constant throughout the whole pathway. We can write an equally true expression for Q considering flow across the second tier alone as:

$$Q = \frac{1}{(1-a)/f(P_2)}(P_1-P_2) \qquad \text{Eqn A8}$$

We then solve Eqn A8 for P_1 in terms of P_2, substitute into Eqn A7 to eliminate P_1, and reduce the rather complex resulting expression to a quadratic equation for Q in terms of a, P_2, and P_0. The appropriate solution is based on:

$$Q = \frac{-B+\sqrt{B^2-4AC}}{2A}$$

(A, B and C are the coefficients of Q^2, Q and constant from the quadratic in Q and have values of:

$$+m[R_0(1-a)]^2,$$

$$R_0[1-mP_2(3-2mP_2+a+amP_2) -P_0m(1+mP_2-a-amP_2)]$$

and

$$-(1+mP_2)^3(P_0-P_2)$$

respectively.)

We used the program Mathematica to evaluate the first and second partial derivatives of Q with respect to both a and P_2 (Abramowitz & Stegun, 1972). The result of this analysis was that the optimal values producing $Q_{\max}$ are $a = 2/3$ and $P_2 = -(2-mP_0)/3m$, where m is the slope of the cavitation function $f(P)$. *These are the same values predicted by the general expressions Eqns A5 and A6 for* n = 2, *which verifies both our inductive logic and that the numerical solutions are effectively identifying true optima for the multi-tiered pathways.*

4. *Matric flux and* n = ∞

When $n = \infty$ we can use the matric flux integration as shown in Eqn 8. The definite integral in terms of P_0 and $P_{@K=0}$ expands to:

$$Q^*_{\max} = K_0[P_0(1+mP_0)-P_{@K=0}(1+0.5mP_{@K=0}) \qquad \text{Eqn A9}$$

This reduces to:

$$Q^*_{\max} = K_0[1+0.5mP_{@K=0}+P_0)](P_0-P_{@K=0}) \qquad \text{Eqn A10}$$

We note that for linear $f(P)$, $P_{@K=0} = -1/m$. We can substitute this in replacing $P_{@K=0}$ in the middle factor only, and giving us Eqn 9 in the main text. Note that the third factor is ΔP, and Eqn A10 predicts that the gradient should reach the point of causing 100% cavitation at the distal endpoint of the gradient. This is consistent with Eqn A5 in the limit where n goes to infinity.

5. R_{pit}, *variable pathway resistance and OCLD*

A fully explicit statement equivalent to Eqn A6 is:

$$\frac{\int_{l(i-1)}^{l_i} R_{\text{lumen}}(l)\,\mathrm{d}l + R_{\text{pit}}}{R_0} = \frac{2}{n}\left[1-\frac{i}{(n+1)}\right] \qquad \text{Eqn A11a}$$

($R_{\text{lumen}}(l)$ can be any continuous function describing variation in lumen resistivity per unit length in different parts of the flow pathway; R_{pit} is expected to be quite small relative to the integral term, and consequently has only a minor influence on the tier-length distribution.) In general, it will have a greater relative importance in short tiers where the integral term is smaller, and therefore including R_{pit} in the analysis causes the length difference predicted between basal and distal tiers to be greater. However, the total effect is rather small. In the restrictive case where $R_{\text{lumen}}(l)$ is a constant:

$$L_i = \frac{2}{n}\frac{R_0[1-i/(n+1)]-R_{\text{pit}}}{R_{\text{lumen}}(l)} \qquad \text{Eqn A11b}$$

6. *Proof of Eqn* 15 *describing limited cavitation containment*

We define this limitation, $\Theta(n)$, to be $1 - Q_{\max}(n)/Q_{\max}(@n = \infty)$, where $Q_{\max}(@n = \infty)$ is calculated as $Q^*_{\max}$ as defined by Eqn 8. This limitation arises from a failure to restrict cavitation to its points of origin in the pathway, and declines as the partitioning of the pathway increases with increasing n.

We begin our proof by showing that Eqn A3, developed for the single-tiered pathway, also holds in identical form for the two-tiered pathway, and infer that the expected level of overall conductance loss from cavitation in the pathway at $Q_{\max}$ is independent of n as long as the pathway has an OCLD.

We begin by restating that, for $n = 2$:

$$\frac{K}{K_0} = \frac{R_0}{R} = \frac{R_0}{R_0[a/f(P_1)+(1-a)/f(P_2)]} \qquad \text{Eqn A12}$$

Again, we wish to proceed by first eliminating P_1. This time we can use a simpler strategy than using Eqn 8, because we are deriving an expression that is true only in the limit of $Q_{\max}$, and not generally for any value of Q. The short-cut is to recognize that, at $Q_{\max}$, the distal tier will behave exactly as a single-tiered pathway would, with P_1 as its input pressure. This allows us to use Eqn 6 to formulate the substitution $P_1 = (2mP_2+1)/m$. Using this expression allows us to reduce A12 to:

$$\frac{K}{K_0} = \frac{2(1+mP_2)}{2-a} \qquad \text{Eqn A13}$$

We now make a second set of substitutions using the optimal values from the analytic solution at $n = 2$ of $a = 2/3$, and $P_2 = -(2-mP_0)/3m$; algebraically reduce; and conclude that, at $Q_{\max}$:

$$\frac{K}{K_0} = 0.5(1+mP_0)$$

This is identical to Eqn A3 (for $n = 1$) and to the middle factor of A10 (for $n = \infty$). This tells us that the expected level of cavitation at $Q_{\max}$ is a constant with respect to n, a result consistent with our numeric model results for all n. By Ohm's law, all variation in $Q_{\max}$ with n must therefore be related to variation in P_n and ΔP. Recognizing that, for our linear $f(P)$, P at the 100% conductance loss point ($P_{k=0}$) has the value $-1/m$, we therefore write:

$$\Theta(n) = 1-\frac{Q_{\max}(n)}{Q_{\max}(\infty)} = 1-\frac{P_0-P_n}{P_o+1/m} \qquad \text{Eqn A14}$$

Substituting from Eqn A5 for P_n, we finally derive Eqn 15 from the text:

$$\Theta(n) = 1 - \frac{P_0 + (n - mP_0)/(n+1)m}{P_0 + 1/m}$$

$$= 1 - \frac{n}{n+1} = \frac{1}{n+1} \qquad \text{Eqn A15}$$

ACKNOWLEDGEMENTS

We thank Dennis Swaney for his invaluable assistance in solving the two-tiered model using Mathematica, and Maurizio Mencuccini and Roman Pausch for helpful comments on the manuscript. During the preparation of this manuscript, the first author was supported in part by NSF grant IBN 94–96093 and USDA 95–37100–1640; the second author was supported in part by NSF grant IBN 9723464 and USDA 97–3700–2649.

REFERENCES

Abramowitz M, Stegun CA. 1972. *Handbook of mathematical functions with formulas, graphs, and mathematical tables*. New York, USA: Dover.

Aloni R, Alexander JD, Tyree MT. 1997. Natural and experimentally altered hydraulic architecture of branch junctions in *Acer saccharum* Marsh. and *Quercus velutina* Lam. trees. *Trees* **11**: 255–264.

Aloni R, Griffith M. 1991. Functional xylem anatomy in root–shoot junctions of six cereal species. *Planta* **184**: 123–129.

Baas P. 1982. Systematic, phylogenetic, and ecological wood anatomy: history and perspectives. In: Baas P, ed. *New perspectives in wood anatomy*. The Hague, The Netherlands: Nijhoff/Junk, 23–58.

Baas P. 1986. Ecological patterns in xylem anatomy. In: Givnish TJ, ed. *On the economy of plant form and function*. New York, USA: Cambridge University Press, 327–351.

Bailey IW. 1953. Evolution of the tracheary tissue of land plants. *American Journal of Botany* **40**: 4–8.

Bailey IW, Tupper WW. 1918. Size variation in tracheary cells. I. A comparison between the secondary xylems of vascular cryptogams, gymnosperms, and angiosperms. *Proceedings of the Academy of American Arts and Sciences* **54**: 149–204.

Barghoon ES. 1964. Evolution of the cambium in geological time. In: Zimmermann MH, ed. *The formation of wood in forest trees*. New York, USA: Academic Press, 3–17.

Bateman RM, Crane PR, DiMichele WA, Kenrick PR, Rowe NP, Speck T, Stein WE. 1998. Early evolution of land plants: phylogeny, physiology, and ecology of the primary terrestrial radiation. *Annual Review of Ecology and Systematics* **29**: 263–292.

Buchmueller KS. 1986. Characteristics of annual rings and vessel lengths of *Fagus sylvatica*. *Vierteljahrsschrift Der Naturforschenden Gesellschaft in Zürich* **131**: 161–182.

Calkin HW, Gibson AC, Nobel PS. 1986. Biophysical model of xylem conductance in tracheids of the fern *Pteris vittata*. *Journal of Experimental Botany* **37**: 1054–1064.

Campbell GS. 1985. *Soil physics with basic transport models for soil plant systems*. New York, USA: Elsevier Science Publishers.

Carlquist S. 1975. *Ecological strategies of xylem evolution*. Berkeley, CA, USA: University of California Press.

Chiu ST, Ewers FW. 1992. Xylem structure and water transport in a twiner, a scrambler, and a shrub of *Lonicera* (Caprifoliaceae). *Trees* **6**: 216–224.

Chiu ST, Ewers FW. 1993. The effect of segment length on conductance measurements in *Lonicera fragrantissima*. *Journal of Experimental Botany* **44**: 175–181.

Cochard H, Breda N, Granier A. 1995. Whole tree hydraulic conductance and water loss regulation in *Quercus* during drought: evidence for stomatal control of embolism? *Annales des Sciences Forestières* **53**: 197–206.

Cochard H, Breda N, Granier A, Aussenac G. 1992. Vulnerability to air embolism of three European oak species: *Quercus petraea* Matt Liebl, *Quercus pubescens* Willd, *Quercus robur* L. *Annales des Sciences Forestières* **49**: 225–233.

Crombie DS, Hipkins MF, Milburn JA. 1985. Gas penetration of pit membranes in the xylem of *Rhododendron* as the cause of acoustically detectable sap cavitation. *Australian Journal of Plant Physiology* **12**: 445–453.

Cronquist A. 1988. *The evolution and classification of flowering plants*. Bronx, New York, USA: The New York Botanical Garden.

Davis SD, Sperry JS, Hacke UG. 1999. The relationship between xylem conduit diameter and cavitation caused by freezing. *American Journal of Botany* **86**: 1367–1372.

Doyle JA. 1998. Phylogeny of vascular plants. *Annual Review of Ecology and Systematics* **29**: 567–599.

Edwards D. 1993. Tansley Review No. 53. Cells and tissues in the vegetative sporophytes of early land plants. *New Phytologist* **125**: 225–247.

Edwards D. 1996. New insights into early land ecosystems: a glimpse of a Lilliputian world. *Review of Palaeobotany and Palynology* **90**: 159–174.

Edwards D, Davies ECW. 1976. Oldest recorded *in situ* tracheids. *Nature* **263**: 494–496.

Ellmore GS, Ewers FW. 1986. Fluid flow in the outermost xylem increment of a ring-porous tree, *Ulmus americana*. *American Journal of Botany* **73**: 1771–1774.

Ewers FW. 1985. Xylem structure and water conduction in conifer trees, dicot trees, and lianas. *International Association of Wood Anatomists Bulletin* **6**: 309–317.

Ewers FW, Carlton MR, Fisher JB, Kolb KJ, Tyree MT. 1997. Vessel diameters in roots versus stems of tropical lianas and other growth forms. *International Association of Wood Anatomists* (*IAWA*) *Journal* **18**: 261–279.

Ewers FW, Cruziat P. 1991. Measuring water transport and storage. In: Lassoie JP, Hinckley TM, eds. *Techniques and approaches in forest tree ecophysiology*. Boca Raton, FL, USA: CRC Press, 92–115.

Ewers FW, Fisher JB. 1989a. Techniques for measuring vessel lengths and diameters in stems of woody plants. *American Journal of Botany* **76**: 645–656.

Ewers FW, Fisher JB. 1989b. Variation in vessel length and diameter in stems of six tropical and subtropical lianas. *American Journal of Botany* **76**: 1452–1459.

Ewers FW, Fisher JB. 1991. Why vines have narrow stems: histological trends in *Bauhinia fabaceae*. *Oecologia* **88**: 233–237.

Ewers FW, Fisher JB, Chiu ST. 1990. A survey of vessel dimensions in stems of tropical lianas and other growth forms. *Oecologia* **84**: 544–552.

Ewers FW, Fisher JB, Fichtner K. 1991. Water flux and xylem structure in vines. In: Putz FE, Mooney H, eds. *Biology of vines*. Cambridge, UK: Cambridge University Press, 119–152.

Ewers FW, Zimmerman MH. 1984. The hydraulic architecture of eastern hemlock, *Tsuga canadensis*. *Canadian Journal of Botany* **62**: 940–946.

Fisher JB, Ewers FW. 1995. Vessel dimensions in liana and tree species of *Gnetum* (Gnetales). *American Journal of Botany* **82**: 1350–1357.

Gibson AC, Calkin HW, Nobel PS. 1984. Xylem anatomy, water flow, and hydraulic conductance in the fern *Cyrtomium falcatum*. *American Journal of Botany* **71**: 564–574.

Gifford EM, Foster AS. 1989. *Morphology and evolution of vascular plants, 3rd edn*. New York, USA: W. H. Freeman.

Greenidge KNH. 1952. An approach to the study of vessel length in hardwood species. *American Journal of Botany* **39**: 570–574.

Grew N. 1682. *The anatomy of plants. With an idea of a philosophical history of plants and several other lectures read before the Royal Society*. London, UK: W. Rawlins.

Gross GG. 1980. The biochemistry of lignification. *Advances in Botanical Research* **8**: 25–63.

Hacke U, Sauter JJ. 1995. Vulnerability of xylem to embolism in relation to leaf water potential and stomatal conductance in *Fagus sylvatica*, *F. purpurea* and *Populus balsamifera*. *Journal of Experimental Botany* **46**: 1177–1183.

Hacke UG, Sperry JS, Ewers BE, Ellsworth DS, Schafer KVR, Oren R. 2000. Influence of soil porosity on water use in *Pinus taeda*. *Oecologia* **124**: 495–505.

Hammel HT. 1967. Freezing of xylem sap without cavitation. *Plant Physiology* **42**: 55–66.

Handley WRC. 1936. Some observations on the problems of vessel length determination in woody dicotyledons. *New Phytologist* **35**: 456–471.

Hargrave KR, Kolb KJ, Ewers FW, Davis SD. 1994. Conduit diameter and drought-induced embolism in *Salvia mellifera* Greene (Labiatae). *New Phytologist* **126**: 695–705.

Jarbeau J, Ewers FW, Davis SD. 1995. The mechanism of water stress induced embolism in two species of chaparral shrubs. *Plant, Cell & Environment* **18**: 189–196.

Jones HG, Sutherland RA. 1991. Stomatal control of xylem embolism. *Plant, Cell & Environment* **14**: 607–612.

Joyce BJ, Steiner KC. 1995. Systematic variation in xylem hydraulic capacity within the crown of white ash (*Fraxinus americana*). *Tree Physiology* **15**: 649–656.

Kenrick P, Crane PR. 1997. *The origin and early diversification of land plants: a cladistic study*. Washington, DC, USA: Smithsonian Institution Press.

Kolb KJ, Sperry JS. 1999a. Differences in drought adaptation between subspecies of sagebrush (*Artemisia tridentata*). *Ecology* **80**: 2373–2384.

Kolb KJ, Sperry JS. 1999b. Transport constraints on water use by the Great Basin shrub, *Artemisia tridentata*. *Plant, Cell & Environment* **22**: 925–935.

Legge NJ. 1985. Anatomical aspects of water movement through stems of mountain ash (*Eucalyptus regnans* F. Muell.). *Australian Journal of Botany* **33**: 287–298.

Linton MJ, Nobel PS. 1999. Loss of water transport capacity due to xylem cavitation in roots of two CAM succulents. *American Journal of Botany* **86**: 1538–1543.

Linton MJ, Sperry JS, Williams DG. 1998. Limits to water transport in *Juniperus osteosperma* and *Pinus edulis*: implications for drought tolerance and regulation of transpiration. *Functional Ecology* **12**: 906–911.

Lo Gullo MA. 1989. Xylem architecture as the anatomical basis of drought resistance in the desert shrub *Simmondsia chinensis* Link Schneider. *Giornale Botanico Italiano* **123**: 255–268.

Lo Gullo MAL, Salleo S. 1993. Different vulnerabilities of *Quercus ilex* L. to freeze- and summer drought-induced xylem embolism: an ecological interpretation. *Plant, Cell & Environment* **16**: 511–519.

Lo Gullo MA, Salleo S, Piaceri EC, Rosso R. 1995. Relations between vulnerability to xylem embolism and xylem conduit dimensions in young trees of *Quercus cerris*. *Plant, Cell & Environment* **18**: 661–669.

Lu P, Biron P, Granier A, Cochard H. 1996. Water relations of adult Norway spruce (*Picea abies* (L.) Karst) under soil drought in the Vosges mountains: whole-tree hydraulic conductance, xylem embolism and water loss regulation. *Annales des Sciences Forestières* **53**: 113–121.

Mauseth JD. 1988. *Plant anatomy*. Menlo Park, CA, USA: Benjamin Cummings.

Meinzer FC, Andrade JL, Goldstein G, Holbrook NM, Cavelier J, Jackson P. 1997. Control of transpiration from the upper canopy of a tropical forest: the role of stomatal, boundary layer and hydraulic architecture components. *Plant, Cell & Environment* **20**: 1242–1252.

Meinzer FC, Goldstein G, Neufeld HS, Grantz DA, Crisosto GM. 1992. Hydraulic architecture of sugarcane in relation to patterns of water use during plant development. *Plant, Cell & Environment* **15**: 471–477.

Mencuccini M, Comstock J. 1997. Vulnerability to cavitation in populations of two desert species, *Hymenoclea salsola* and *Ambrosia dumosa*, from different climatic regions. *Journal of Experimental Botany* **48**: 1323–1334.

Neufeld HS, Grantz DA, Meinzer FC, Goldstein G, Crisosto GM, Crisosto C. 1992. Genotypic variability in vulnerability of leaf xylem to cavitation in water-stressed and well-irrigated sugarcane. *Plant Physiology* **100**: 1020–1028.

Niklas KJ. 1985. The evolution of tracheid diameter in early vascular plants and its implications on the hydraulic conductance of the primary xylem strand. *Evolution* **39**: 1110–1122.

Niklas KJ. 1997. *The evolutionary biology of plants*. Chicago, IL, USA: University of Chicago Press.

Oertli JJ. 1971. The stability of water under tension in the xylem. *Zeitschrift für Pflanzenphysiologie* **65**: 195–209.

Pallardy SG. 1989. Hydraulic architecture and conductivity, an overview. In: Kreeb KH, Richter H, Hinckley TM, eds. *Structural and functional responses to environmental stresses: water shortage*. The Hague, The Netherlands: SPB Academic Publishing, 3–20.

Passioura JB. 1988. Water transport in and to roots. *Annual Review of Plant Physiology and Plant Molecular Biology* **39**: 245–265.

Pickard WF. 1981. The ascent of sap in plants. *Progress in Biophysics and Molecular Biology* **37**: 181–229.

Ranasinghe MS, Milburn JA. 1995. Xylem conduction and cavitation in *Hevea brasiliensis*. *Journal of Experimental Botany* **46**: 1693–1700.

Raven JA. 1987. The evolution of vascular land plants in relation to supracellular transport processes. *Advances in Botanical Research* **5**: 153–219.

Saliendra NZ, Sperry JS, Comstock JP. 1995. Influence of leaf water status on stomatal response to humidity, hydraulic conductance, and soil drought in *Betula occidentalis*. *Planta* **196**: 357–366.

Salleo S. 1984. Functional aspects of water conduction pathways in vascular plants. *Giornale Botanico Italiano* **118**: 53–65.

Salleo S, Lo Gullo MA. 1983. Water transport pathways in nodes and internodes of 1-year-old twigs of *Olea europaea*. *Giornale Botanico Italiano* **117**: 63–74.

Salleo S, Lo Gullo MA, Oliveri F. 1985. Hydraulic parameters measured in 1-year-old twigs of some Mediterranean species with diffuse-porous wood changes in hydraulic conductivity and their possible functional significance. *Journal of Experimental Botany* **36**: 1–11.

Schulte PJ, Gibson AC. 1987. Hydraulic conductance and tracheid anatomy in six species of extant seed plants. *Canadian Journal of Botany* **66**: 1073–1079.

Schulte PJ, Gibson AC, Nobel PS. 1987. Xylem anatomy and hydraulic conductance of *Psilotum nudum*. *American Journal of Botany* **74**: 1438–1445.

Sellin AA. 1988. Hydraulic architecture in the Norway spruce. *Fiziologiya Rastenii* **35**: 1099–1107.

Sparks JP, Black RA. 1999. Regulation of water loss in populations of *Populus trichocarpa*: the role of stomatal control in preventing xylem cavitation. *Tree Physiology* **19**: 453–459.

Sperry JS. 1986. Relationship of xylem embolism to xylem pressure potential stomatal closure and shoot morphology in the palm *Rhapis excelsa*. *Plant Physiology* **80**: 110–116.

Sperry JS. 1995. Limitations on stem water transport and their consequences. In: Gartner BL, ed. *Plant stems: physiology and functional morphology*. New York, USA: Academic Press, 105–124.

Sperry JS, Adler FR, Campbell GS, Comstock JP. 1998. Limitation of plant water use by rhizosphere and xylem conductance: results from a model. *Plant, Cell & Environment* **21**: 347–359.

Sperry JS, Alder NN, Eastlack SE. 1993. The effect of reduced hydraulic conductance on stomatal conductance and xylem cavitation. *Journal of Experimental Botany* **44**: 1075–1082.

Sperry JS, Ikeda T. 1997. Xylem cavitation in roots and stems of Douglas-fir and white fir. *Tree Physiology* **17**: 275–280.

Sperry JS, Nichols LK, Sullivan JEM, Eastlack SE. 1994. Xylem embolism in ring-porous, diffuse-porous, and coniferous trees of northern Utah and interior Alaska. *Ecology* **75**: 1736–1752.

Sperry JS, Saliendra NZ. 1994. Intra- and inter-plant variation in xylem cavitation in *Betula occidentalis*. *Plant, Cell & Environment* **17**: 1233–1241.

Sperry JS, Saliendra NZ, Pockman WT, Cochard H, Cruziat P, Davis SD, Ewers FW, Tyree MT. 1996. New evidence for large negative xylem pressures and their measurement by the pressure chamber method. *Plant, Cell & Environment* **19**: 426–436.

Sperry J, Tyree M. 1988. Mechanism of water-stress induced xylem embolism. *Plant Physiology* **88**: 581–587.

Sperry JS, Tyree MT. 1990. Water-stress-induced xylem embolism in three species of conifers. *Plant, Cell & Environment* **13**: 427–436.

Tognetti R, Borghetti M. 1994. Formation and seasonal occurrence of xylem embolism in *Alnus cordata*. *Tree Physiology* **14**: 241–250.

Tsuda M, Tyree MT. 1997. Whole-plant hydraulic resistance and vulnerability segmentation in *Acer saccharinum*. *Tree Physiology* **17**: 351–357.

Tyree MT. 1992. Theory of vessel-length determination: the problem of non-random vessel ends. *Canadian Journal of Botany* **71**: 297–302.

Tyree MT. 1997. The cohesion–tension theory of sap ascent: current controversies. *Journal of Experimental Botany* **48**: 1753–1765.

Tyree MT, Cochard H, Cruziat P, Sinclair B, Ameglio T. 1993. Drought-induced leaf shedding in walnut: evidence for vulnerability segmentation. *Plant, Cell & Environment* **16**: 879–882.

Tyree MT, Davis SD, Cochard H. 1994a. Biophysical perspectives of xylem evolution: is there a tradeoff of hydraulic efficacy for vulnerability to dysfunction? *International Association of Wood Anatomists* (*IAWA*) *Journal* **15**: 335–360.

Tyree MT, Ewers FW. 1991. Tansley Review No. 34: The hydraulic architecture of trees and other woody plants. *New Phytologist* **119**: 345–360.

Tyree MT, Kolb KJ, Rood SB, Patino S. 1994b. Vulnerability to drought-induced cavitation of riparian cottonwoods in Alberta: a possible factor in the decline of the ecosystem? *Tree Physiology* **14**: 455–466.

Tyree MT, Sperry JS. 1988. Do woody plants operate near the point of catastrophic xylem dysfunction caused by dynamic water stress? *Plant Physiology* **88**: 574–580.

Tyree MT, Sperry JS. 1989. Vulnerability of xylem to cavitation and embolism. *Annual Review of Plant Physiology and Plant Molecular Biology* **40**: 19–38.

Veres JS. 1990. Xylem anatomy and hydraulic conductance of Costa Rican blechnum ferns. *American Journal of Botany* **77**: 1610–1625.

Vogel S. 1988. *Life's devices*. Princeton, NJ, USA: Princeton University Press.

Yang S, Tyree MT. 1993. Hydraulic resistance in *Acer saccharum* shoots and its influence of leaf water potential and transpiration. *Tree Physiology* **12**: 231–242.

Yang S, Tyree MT. 1994. Hydraulic architecture of *Acer saccharum* and *A. rubrum*: comparison of branches to whole trees and the contribution of leaves to hydraulic resistance. *Journal of Experimental Botany* **45**: 179–186.

Zimmermann MH. 1978. Vessel ends and the disruption of water flow in plants. *Phytopathology* **68**: 253–255.

Zimmermann MH. 1982. *Functional xylem anatomy of angiosperm trees*. The Hague, The Netherlands: Dr W. Junk Publishers.

Zimmermann MH. 1983. *Xylem structure and the ascent of sap*. Berlin, Germany: Springer-Verlag.

Zimmermann MH, Brown CL. 1971. *Trees: structure and function*. New York, USA: Springer-Verlag.

Zimmermann MH, Jeje AA. 1981. Vessel-length distribution of some American woody plants. *Canadian Journal of Botany* **59**: 1882–1892.

Zimmermann MH, McCue KF, Sperry JS. 1982. Anatomy of the palm *Rhapsis excelsa*. VIII. Vessel network and vessel-length distribution in the stem. *Journal of the Arnold Arboretum* **63**: 83–93.

Zimmermann MH, Potter D. 1982. Vessel-length distribution in branches, stem, and roots of *Acer rubrum*. *International Association of Wood Anatomists* (*IAWA*) *Bulletin* **3**: 103–109.

Zotz G, Tyree MT, Patiño S. 1997. Hydraulic architecture and water relations of a flood-tolerant tropical tree, *Annona glabra*. *Tree Physiology* **17**: 359–365.